Transverse momentum dependence of the angular distribution of the Drell-Yan process

Edmond L. Berger,[1,*] Jian-Wei Qiu,[1,2,†] and Ricardo A. Rodriguez-Pedraza[2,‡]

[1]*High Energy Physics Division, Argonne National Laboratory, Argonne, Illinois 60439, USA*

[2]*Department of Physics and Astronomy, Iowa State University, Ames, Iowa 50011, USA*

(Received 6 August 2007; revised manuscript received 19 September 2007; published 5 October 2007)

We calculate the transverse momentum $Q_\perp$ dependence of the helicity structure functions for the hadroproduction of a massive pair of leptons with pair invariant mass Q. These structure functions determine the angular distribution of the leptons in the pair rest frame. Unphysical behavior in the region $Q_\perp \to 0$ is seen in the results of calculations done at fixed order in QCD perturbation theory. We use current conservation to demonstrate that the unphysical inverse-power and $\ln(Q/Q_\perp)$ logarithmic divergences in three of the four independent helicity structure functions share the same origin as the divergent terms in fixed-order calculations of the angular-integrated cross section. We show that the resummation of these divergences to all orders in the strong coupling strength α_s can be reduced to the solved problem of the resummation of the divergences in the angular-integrated cross section, resulting in well-behaved predictions in the small $Q_\perp$ region. Among other results, we show the resummed part of the helicity structure functions preserves the Lam-Tung relation between the longitudinal and double spin-flip structure functions as a function of $Q_\perp$ to all orders in α_s.

DOI: 10.1103/PhysRevD.76.074006 PACS numbers: 12.38.Bx, 12.38.Cy, 13.85.Qk

I. INTRODUCTION

Production of a massive pair of leptons of opposite electric charge in hadronic interactions, $h_1 + h_2 \to \ell^+\ell^- X$, has revealed new narrow hadronic states, notably the J/Ψ and the Υ, and it continues to provide an important complement to deep-inelastic lepton scattering and other hard-scattering processes for probing the short-distance dynamics of strong and electroweak interactions. The assumption that the broad continuum of $\ell^+\ell^-$ pairs originates from quark-antiquark annihilation through a single virtual photon, as embodied in the Drell-Yan model [1], implies that the angular distribution in the $\ell^+\ell^-$ rest frame should be that of a transversely polarized photon, $(1 + \cos^2\theta)$, where the polar angle θ is the direction of the lepton relative to the direction of the incident quark and antiquark. Acceptance restrictions limit measurements of the full angular distribution, but qualitative verification of this expectation was one of the early tests that increased confidence in the model [2].

In practice, massive lepton pairs are produced with substantial transverse momentum $Q_\perp$, supplied from a theoretical perspective by higher-order processes in perturbative quantum chromodynamics (QCD). An interesting challenge has been to predict how the angular distribution should behave as a function of $Q_\perp$ [3–11]. Indeed, this challenge is part of the more general ambition to predict the fully differential cross section $d\sigma/dQdQ_\perp dyd\Omega$, where Q is the invariant mass of the lepton pair, y is its rapidity, and $d\Omega = d\cos\theta d\phi$ represents the differential decay angular distribution in the pair rest frame with respect to a suitably chosen set of axes.

In addition to the virtual photon, the W boson and the Z boson also have important decay modes into pairs of leptons. The angular distribution of these leptons, measured in the rest frame of the parent states, determines the alignment (polarization) of the vector boson and, consequently, supplies more precise information on the production dynamics than is accessible from the spin-averaged rate alone. An understanding of the changes expected in the angular distribution as a function of the transverse momentum $Q_\perp$ is a topic of considerable importance, both for refined tests of QCD and for electroweak precision measurements. An example of a QCD process is the flavor dependence of W production in polarized hadron-hadron scattering at the Brookhaven Relativistic Heavy Ion Collider (RHIC) [12]. Better understanding of the expected angular distributions will reduce the systematic uncertainties on the determination of the W boson mass [13,14] and, in turn, improve the bound on the mass of the Higgs boson within the standard model of particle physics.

In this paper we consider the scattering of two hadrons of momentum P_1 and P_2, respectively, producing a virtual photon of four-momentum q, $A(P_1) + B(P_2) \to \gamma^*(q) + X$, that decays into a pair of leptons of momentum l and $\bar{l}$, as sketched in Fig. 1. The ideas and techniques developed here can be applied readily to the production of W and Z bosons, as well as to other yet-to-be-observed massive vector bosons that decay into a pair of leptons. They are applicable also in semi-inclusive deep-inelastic scattering (SIDIS).

The general formalism for the description of the angular distribution in terms of helicity structure functions is developed for the Drell-Yan process in Ref. [4]. The differ-

*berger@anl.gov
†jwq@iastate.edu
‡rirodri@iastate.edu

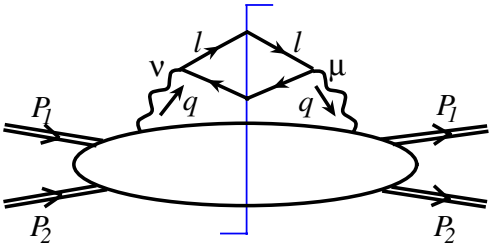

FIG. 1 (color online). Diagrammatic representation of hadronic dilepton production via a virtual photon of four-momentum q.

ential cross section may be expressed as [4]

$$\frac{d\sigma}{d^4q d\Omega} = \frac{\alpha_{\rm em}^2}{2(2\pi)^4 S^2 Q^2}[W_T(1+\cos^2\theta) + W_L(1-\cos^2\theta) + W_\Delta(\sin(2\theta)\cos\phi) + W_{\Delta\Delta}(\sin^2\theta\cos(2\phi))]. \quad (1)$$

The four independent ''helicity'' structure functions W_T, W_L, W_Δ, and $W_{\Delta\Delta}$ depend on Q, $Q_\perp$, rapidity y, and on the center-of-mass energy $\sqrt{S}$ of the production process. They are defined in the virtual photon's rest frame, and they correspond, respectively, to the transverse spin, longitudinal spin, single spin-flip, and double spin-flip contributions to the Drell-Yan cross section.

The angular-integrated cross section is expressed in terms of W_T and W_L as

$$\frac{d\sigma}{d^4q} = \frac{\alpha_{\rm em}^2}{12\pi^3 S^2 Q^2}[2W_T + W_L]. \quad (2)$$

An interesting relationship $W_L = 2W_{\Delta\Delta}$ between the longitudinal and double-flip structure functions is derived in Ref. [4] in the context of the parton model, and it has been shown to hold at least approximately at higher orders in perturbative QCD. Experimental tests of this relationship are reported in Refs. [15–19].

Our principal focus in this paper is the prediction of the full $Q_\perp$ dependence of the four structure functions, including the region of small and intermediate $Q_\perp$ where the cross section takes on its largest values. Many papers dealing with various aspects of Drell-Yan angular distributions have preceded ours. Explicit perturbative calculations were done in the parton model [3,4], in perturbative QCD at order α_s [5–8] and α_s^2 [9], as well as in high twist formalisms [20,21]. When calculated at fixed order in QCD perturbation theory, the structure functions show unphysical inverse-power $Q_\perp^{-n}$ ($n=1$ or 2) or logarithmic $\ln(Q/Q_\perp)$ divergences, or both, as $Q_\perp \to 0$. For the angular-integrated cross section, $d\sigma/d^4q$, it is well established that similar unphysical divergences can be removed after resummation of the $\ln^m(Q^2/Q_\perp^2)/Q_\perp^2$ singular terms from initial-state gluon emission to all orders in α_s [22–25].

Examinations of the singular logarithmic terms in the helicity structure functions are reported in Refs. [10,11,13,14]. Since only W_T shows the $\ln^m(Q^2/Q_\perp^2)/Q_\perp^2$ divergence, previous resummation calculations were carried out only for W_T in the same way as for the angular-integrated cross section. As shown in Refs. [10,13,14], resummation removes the perturbative power divergence in W_T. One consequence of resummation of just W_T is a large change in the relative size of W_T and the helicity structure functions for which no resummation is performed. This result is not quite consistent with general expectations about the relative size of helicity structure functions in the Collins-Soper frame. For example, one expects $W_{\Delta\Delta}/W_T \to Q_\perp^2$ as $Q_\perp \to 0$ [26].

In Ref. [11], Boer and Vogelsang carefully investigate the logarithmic behavior of the order α_s perturbative contributions to the helicity structure functions. At order α_s, they find that, like W_T, both W_L and $W_{\Delta\Delta}$ have a $\ln(Q^2/Q_\perp^2)$ logarithmic divergence, but not the $1/Q_\perp^2$ power divergence seen in W_T, and that W_Δ has no logarithmic divergence at this order in the Collins-Soper frame. They notice that the logarithmic contribution to W_L and $W_{\Delta\Delta}$ from the quark-gluon (or gluon-quark) subprocess is different from that for W_T and does not fit the pattern expected for the perturbative expansion of the Collins-Soper-Sterman resummation formalism to order α_s [25]. They also discuss the frame dependence of this logarithmic contribution.

The present paper expands on our earlier short manuscript on the same subject [27]. We start with the observations that the four helicity structure functions cannot be independent at $Q_\perp = 0$ and that the general tensor decomposition in the virtual photon rest frame in Eq. (4) is ill defined at $Q_\perp = 0$. Then, guided by electromagnetic current conservation, we construct a new asymptotic form for the hadronic tensor with the right degrees of freedom as $Q_\perp \to 0$. We find that the leading logarithmic behavior of the different helicity structure functions, W_T, W_L, and $W_{\Delta\Delta}$, has a unique origin. We reduce the problem of transverse momentum resummation for W_T, W_L, and $W_{\Delta\Delta}$ to the known solution of transverse momentum resummation for the angular-integrated cross section [25], and we prove that the logarithmic divergences in W_T, W_L, and $W_{\Delta\Delta}$ may be resummed to all orders in the strong coupling strength α_s, yielding well-behaved predictions that satisfy the expected kinematic constraints at small $Q_\perp$. We emphasize three main results of our research:

(i) Current conservation uniquely ties the perturbative divergences as $Q_\perp/Q \to 0$ of the otherwise independent helicity structure functions W_T, W_L, and $W_{\Delta\Delta}$ to the divergence of the angular-integrated cross section.

(ii) The perturbative divergence in the angular-integrated cross section is sufficient to remove all leading divergences of the four individual helicity structure functions.

(iii) Transverse momentum resummation of the angular-integrated cross section determines the resummation of the large logarithmic terms of the helicity structure functions W_T, W_L, and $W_{\Delta\Delta}$, and the approximate Lam-Tung relation is an all-orders consequence of current conservation for the leading perturbatively divergent terms.

The rest of our paper is organized as follows. In Sec. II, we define the helicity structure functions, and we derive the QCD perturbative contributions at order α_s. We work in this paper entirely in the context of collinear QCD factorization [28], meaning that $Q_\perp > \Lambda_{\rm QCD}$, although $Q_\perp/Q$ may be small. We examine in detail the leading behavior of the perturbative contributions to the helicity structure functions in the limit of small $Q_\perp/Q$. In Secs. III and IV, we investigate the generic singular structure of the perturbative contribution to the Drell-Yan hadronic tensor, and we derive an asymptotic current-conserving tensor that explicitly includes all the leading divergences of the perturbatively calculated helicity structure functions in the limit $Q_\perp/Q \to 0$. We also explore the connection between cross sections for incident parton states of fixed helicity and the subleading perturbative contribution to the spin-averaged helicity structure functions. We discuss all-orders transverse momentum resummation for helicity structure functions in Sec. V, obtaining well-behaved distributions as a function of $Q_\perp$. We show that the resummed part of the helicity structure functions satisfies the Lam-Tung relation, $W_L = 2W_{\Delta\Delta}$, between the longitudinal and the double spin-flip structure function to all orders in α_s. Finally, in Sec. VI, we offer a summary and our conclusions, and we outline plans for future work on W and Z hadroproduction and in semi-inclusive deep-inelastic scattering. Three appendixes are included in which we present detailed technical derivations of points discussed in the main body of the text.

II. HELICITY STRUCTURE FUNCTIONS AND PERTURBATIVE CONTRIBUTIONS

In this section, we define the helicity structure functions of Eq. (1). We present the next-to-leading order perturbative contributions to these functions and examine the structure of the singular behavior of each helicity structure function W_i as $Q_\perp/Q \to 0$.

A. Definition and normalization

Helicity structure functions are defined in the virtual photon's rest frame. Let $\epsilon^\mu_\lambda(q)$ be the virtual photon's polarization vector with three polarization states, $\lambda = \pm 1, 0$. The helicity structure functions are

$$W_T = W_{\mu\nu}\epsilon_1^{\mu*}\epsilon_1^\nu, \qquad W_L = W_{\mu\nu}\epsilon_0^{\mu*}\epsilon_0^\nu,$$
$$W_\Delta = W_{\mu\nu}(\epsilon_1^{\mu*}\epsilon_0^\nu + \epsilon_0^{\mu*}\epsilon_1^\nu)/\sqrt{2}, \tag{3}$$
$$W_{\Delta\Delta} = W_{\mu\nu}\epsilon_1^{\mu*}\epsilon_{-1}^\nu,$$

for the transverse spin, longitudinal spin, single spin-flip, and double spin-flip contributions to the Drell-Yan cross section, respectively. In the virtual photon rest frame (the center-of-mass frame of the dilepton pair), the polarization vectors can be expressed in terms of orthogonal unit vectors in that frame, X^μ, Y^μ, and Z^μ, as $\epsilon^\mu_\pm = (\mp X^\mu - iY^\mu)/\sqrt{2}$, $\epsilon^\mu_0 = Z^\nu$ [4]. These unit vectors are normalized as $X^2 = Y^2 = Z^2 = -1$, and they are also orthogonal to the current vector q^μ. They conserve the current, $q_\mu X^\mu = q_\mu Y^\mu = q_\mu Z^\mu = 0$. Naturally, we can choose the fourth unit vector for the $\vec{q} = 0$ Lorentz frame to be $T^\mu = q^\mu/Q$ with $T^2 = 1$ and $Q = \sqrt{q^2}$. The full Drell-Yan hadronic tensor can be written in terms of the helicity structure functions and unit vectors in the virtual photon rest frame as [4]

$$\begin{aligned} W^{\mu\nu} = &-(g^{\mu\nu} - T^\mu T^\nu)(W_T + W_{\Delta\Delta}) - 2X^\mu X^\nu W_{\Delta\Delta} \\ &+ Z^\mu Z^\nu (W_L - W_T - W_{\Delta\Delta}) \\ &- (X^\mu Z^\nu + X^\nu Z^\mu) W_\Delta. \end{aligned} \tag{4}$$

Different choices of the axes lead to different $\vec{q} = 0$ frames [4]. We choose to work in the Collins-Soper frame [26], whose unit vectors are defined as

$$\begin{aligned} Z^\mu &= \frac{2}{\sqrt{Q^2 + Q_\perp^2}}[q_{P_2}\tilde{P}_1^\mu - q_{P_1}\tilde{P}_2^\mu], \\ X^\mu &= -\left(\frac{Q}{Q_\perp}\right)\frac{2}{\sqrt{Q^2 + Q_\perp^2}}[q_{P_2}\tilde{P}_1^\mu + q_{P_1}\tilde{P}_2^\mu], \\ Y^\mu &= \epsilon^{\mu\nu\alpha\beta}T_\nu Z_\alpha X_\beta, \end{aligned} \tag{5}$$

where the dimensionless current-conserving hadron momenta are $\tilde{P}_i^\mu = [P_i^\mu - (P_i \cdot q)/q^2 q^\mu]/\sqrt{S}$ with $i = 1, 2$, and $q_{P_i} \equiv P_i \cdot q/\sqrt{S}$ with $i = 1, 2$. We present our derivation and predictions on helicity structure functions in this Collins-Soper frame. Transformation of our results to other commonly used frames is simply a rotation around the Y axis [4,11].

When the virtual photon mass Q and its transverse momentum $Q_\perp$ are much larger than $\Lambda_{\rm QCD}$, we expect QCD collinear factorization to be valid for the Drell-Yan cross section [28]. Neglecting the transverse momentum of partons participating in the hard collisions, we write the incident parton momenta as

$$p_1^\mu = \xi_1 P_1^\mu; \qquad p_2^\mu = \xi_2 P_2^\mu. \tag{6}$$

Neglecting all corrections suppressed by powers of $\Lambda_{\rm QCD}/Q$ or $\Lambda_{\rm QCD}/Q_\perp$, we can factor the hadronic tensor as

$$W^{\mu\nu} = \sum_{ab} \int \frac{d\xi_1}{\xi_1} \times \int \frac{d\xi_2}{\xi_2} \phi_a(\xi_1)\phi_b(\xi_2)\omega^{\mu\nu}_{ab\to\gamma^* X}(\xi_1, \xi_2, q), \quad (7)$$

with incoming parton distributions $\phi_f(\xi)$ of flavor f and momentum fraction ξ. The short-distance partonic tensor is

$$\omega^{\mu\nu}_{ab\to\gamma^* X} = S\overline{\sum}|M^{\mu}_{ab\to\gamma^* X}|^*|M^{\nu}_{ab\to\gamma^* X}|(2\pi)^4 \times \delta^4(p_1 + p_2 - q - \sum_x p_x)\prod_x \frac{d^3p_x}{(2\pi)^3 2E_x}. \quad (8)$$

At the most basic level, a massive virtual photon arises from quark-antiquark annihilation $q + \bar{q} \to \gamma^*$ in a collision of hadrons, and it is produced with $Q_\perp = 0$. The corresponding partonic tensor is

$$\omega^{\mu\nu}_{q\bar{q}\to\gamma^*} = \tfrac{1}{3}e_q^2[\bar{n}^\mu n^\nu + n^\mu \bar{n}^\nu - g^{\mu\nu}]\xi_1\xi_2\delta(\xi_1 - x_1) \times \delta(\xi_2 - x_2)(2\pi)^4 S\delta^2(Q_\perp), \quad (9)$$

with color factor $1/3$ and fractional quark charge e_q. The unit vectors are $\bar{n}^\mu = \delta^{\mu+}$ and $n^\mu = \delta^{\mu-}$, and

$$x_1 = \frac{Q}{\sqrt{S}}e^{y}, \qquad x_2 = \frac{Q}{\sqrt{S}}e^{-y}. \quad (10)$$

The lowest order helicity structure functions from $q\bar{q} \to \gamma^*$ are

$$W_T^{(0)} = \sum_q \frac{1}{3}e_q^2\phi_q(x_1)\phi_{\bar{q}}(x_2)(2\pi)^4 S\delta^2(Q_\perp), \qquad W_L^{(0)} = W_\Delta^{(0)} = W_{\Delta\Delta}^{(0)} = 0. \quad (11)$$

First-order gluon radiation supplies finite $Q_\perp$, through the quark-antiquark and quark-gluon subprocesses, $q + \bar{q} \to \gamma^* + g$ and $q + g \to \gamma^* + q$, as sketched in Figs. 2 and 3, respectively. Perturbatively, these finite-order subprocesses yield *singular* differential cross sections as a function of $Q_\perp$ in the limit $Q_\perp/Q \to 0$. For the angular-integrated cross section, $d\sigma/d^4q$, it is well established that this unphysical divergence can be removed after resummation of the singular terms from initial-state gluon emission to all orders in α_s [25]. The dependence of the helicity structure functions on $Q_\perp$ is our central focus in the rest of this manuscript.

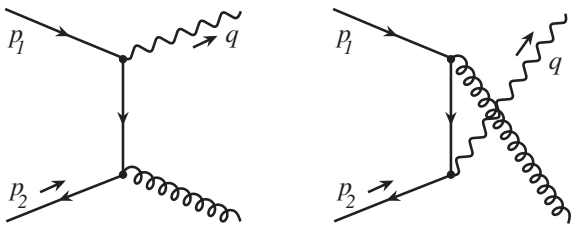

FIG. 2. Feynman diagrams for quark-antiquark annihilation to a virtual photon plus a gluon.

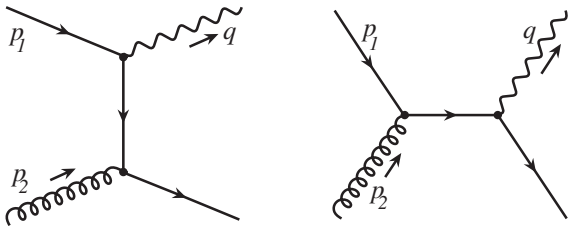

FIG. 3. Feynman diagrams for quark-gluon scattering to produce a virtual photon plus a quark.

B. Order α_s contribution

In this section we present explicit expressions for the contributions at order α_s to the four helicity structure functions from the two subprocesses $q\bar{q} \to \gamma^* g$ and $qg \to \gamma^* q$. Although some of the perturbative results are available in the literature, we present for completeness, in Appendixes B and C, the details of the perturbative calculation in a consistent notation for the spin-averaged and ''polarized'' contributions to the parton-level helicity structure functions in the Collins-Soper frame.

To better identify the analytic behavior as $Q_\perp/Q \to 0$ of the perturbative contributions, we express the results in terms of two new variables,

$$z_1 \equiv \frac{x_1}{\xi_1}, \qquad z_2 \equiv \frac{x_2}{\xi_2}. \quad (12)$$

The parton-level Mandelstam variables defined in Eq. (B3) in Appendix B are expressed as

$$\hat{s} = \frac{Q^2}{z_1 z_2}, \qquad \hat{t} = -\frac{Q_\perp^2}{1 - z_2\sqrt{1 + Q_\perp^2/Q^2}}, \qquad \hat{u} = -\frac{Q_\perp^2}{1 - z_1\sqrt{1 + Q_\perp^2/Q^2}}, \quad (13)$$

and

$$\frac{1}{\hat{t}\,\hat{u}} = \frac{1}{\hat{s}Q_\perp^2}, \qquad \frac{1}{\hat{s}(-\hat{t})} = \frac{1}{\hat{s}Q_\perp^2}[1 - z_2\sqrt{1 + Q_\perp^2/Q^2}].$$

In the following subsections, we present our calculation for spin-averaged and polarized incident partons, with our specification of polarized states presented below.

1. Spin-averaged quark-antiquark annihilation

As derived in Eq. (B5) in Appendix B, the contributions to the parton-level helicity structure functions from the quark-antiquark annihilation subprocess, after averaging over the spins of the incident quark and antiquark, are

$$
\begin{aligned}
w_T^{q\bar{q}} &= e_q^2 \frac{8\pi^2\alpha_s}{3}\left(\frac{Q^2}{Q_\perp^2}\right)C_F[z_1^2+z_2^2]\left(1+\frac{1}{2}\frac{Q_\perp^2}{Q^2}\right)\frac{S}{z_1 z_2}\delta(\hat{s}+\hat{t}+\hat{u}-Q^2),\\
w_L^{q\bar{q}} &= e_q^2 \frac{8\pi^2\alpha_s}{3}C_F[z_1^2+z_2^2]\frac{S}{z_1 z_2}\delta(\hat{s}+\hat{t}+\hat{u}-Q^2),\\
w_{\Delta\Delta}^{q\bar{q}} &= e_q^2 \frac{8\pi^2\alpha_s}{3}\frac{1}{2}C_F[z_1^2+z_2^2]\frac{S}{z_1 z_2}\delta(\hat{s}+\hat{t}+\hat{u}-Q^2) = \frac{1}{2}w_L^{q\bar{q}},\\
w_\Delta^{q\bar{q}} &= e_q^2 \frac{8\pi^2\alpha_s}{3}\left(\frac{Q}{Q_\perp}\right)C_F[z_1^2-z_2^2]\frac{S}{z_1 z_2}\delta(\hat{s}+\hat{t}+\hat{u}-Q^2).
\end{aligned}
\tag{14}
$$

The color factor is written as $4/9 = (1/3)\times C_F$, with $(1/3)$ being the color factor for the lowest order contribution in Eq. (9), and $C_F = 4/3$. With the exchange of z_1 and z_2 (or $\hat{t}$ and $\hat{u}$), Eq. (14) is also valid for the antiquark-quark scattering subprocess, except for $w_\Delta^{\bar{q}q}$ which acquires an extra overall minus sign that arises from the minus sign in the expression for w_Δ in Eq. (A12).

The phase space δ function can also be expressed in terms of the new variables as

$$
\begin{aligned}
\frac{S}{z_1 z_2}\delta(\hat{s}+\hat{t}+\hat{u}-Q^2) = \frac{1}{x_1 x_2}\delta\Bigg(&\left(1-z_1\sqrt{1+Q_\perp^2/Q^2}\right)\\
&\times\left(1-z_2\sqrt{1+Q_\perp^2/Q^2}\right)-Q_\perp^2/\hat{s}\Bigg).
\end{aligned}
\tag{15}
$$

2. Spin-averaged quark-gluon scattering

As derived in Eq. (B8) in Appendix B, the contributions from the quark-gluon subprocess, after an average over the spins of the initial quark and gluon, are

$$
\begin{aligned}
w_T^{qg} &= e_q^2 \frac{8\pi^2\alpha_s}{3}\left(\frac{Q^2}{Q_\perp^2}\right)\left[1-z_2\sqrt{1+Q_\perp^2/Q^2}\right]T_R\left[[z_2^2+(z_1z_2-1)^2]+\frac{1}{2}\frac{Q_\perp^2}{Q^2}[z_2^2-(z_1+z_2)^2]\right]\frac{S}{z_1 z_2}\delta(\hat{s}+\hat{t}+\hat{u}-Q^2),\\
w_L^{qg} &= e_q^2 \frac{8\pi^2\alpha_s}{3}\left[1-z_2\sqrt{1+Q_\perp^2/Q^2}\right]T_R[z_2^2+(z_1+z_2)^2]\frac{S}{z_1 z_2}\delta(\hat{s}+\hat{t}+\hat{u}-Q^2),\\
w_{\Delta\Delta}^{qg} &= e_q^2 \frac{8\pi^2\alpha_s}{3}\left[1-z_2\sqrt{1+Q_\perp^2/Q^2}\right]\frac{1}{2}T_R[z_2^2+(z_1+z_2)^2]\frac{S}{z_1 z_2}\delta(\hat{s}+\hat{t}+\hat{u}-Q^2) = \frac{1}{2}w_L^{qg},\\
w_\Delta^{qg} &= e_q^2 \frac{8\pi^2\alpha_s}{3}\left(\frac{Q}{Q_\perp}\right)\left[1-z_2\sqrt{1+Q_\perp^2/Q^2}\right]T_R[z_1^2-2z_2^2]\frac{S}{z_1 z_2}\delta(\hat{s}+\hat{t}+\hat{u}-Q^2).
\end{aligned}
\tag{16}
$$

The color factor is written as $1/6 = (1/3)\times T_R$ with $T_R = 1/2$. With z_1 and z_2 switched, Eq. (16) is also true for the gluon-quark scattering subprocesses, except for w_Δ^{gq} which acquires an extra overall minus sign that arises from the minus sign in the expression for w_Δ in Eq. (A12).

3. Expressions for polarized incident partons

The behavior at small $Q_\perp/Q$ of the parton-level helicity structure functions is sensitive to the helicity states of the incoming partons. We present here the perturbative contribution to the helicity structure functions from the $q+\bar{q}\to\gamma^*+g$ and $q+g\to\gamma^*+q$ subprocesses with an initial-state (anti)quark and gluon in a fixed helicity state. For a quark of momentum p, the helicity projection operator is

$$
\hat{P}_\pm(p) = \tfrac{1}{2}\gamma\cdot p \pm \tfrac{1}{2}\gamma\cdot p\gamma_5, \tag{17}
$$

where the first term on the right-hand side (RHS) corresponds to the projection for a spin-averaged quark state, while the second term corresponds to the projection for a polarized quark state, defined as the state with incoming quark polarization projected onto the *difference* of the quark's helicity states. Similarly, the helicity projection operator for a massless gluon of momentum p moving in either the light-cone "+" or "−" direction is

$$
P_\pm^{\alpha\beta}(p) = \tfrac{1}{2}d^{\alpha\beta} \pm \tfrac{1}{2}i\epsilon^{\alpha\beta}, \tag{18}
$$

where the transverse tensor $d^{\alpha\beta} = -g^{\alpha\beta}+\bar{n}^\alpha n^\beta + n^\alpha\bar{n}^\beta$, $\epsilon^{\alpha\beta} = \epsilon^{\alpha\beta\rho\sigma}\bar{n}_\rho n_\sigma$. The first term on the RHS again corresponds to the projection for a spin-averaged and physically polarized gluon state, while the second term corresponds to the projection to a polarized gluon state, defined as the state with incoming gluon polarization projected onto the *difference* of the gluon's physically polarized states.

The contribution with a mixed unpolarized and a polarized parton state leads to an antisymmetric contribution to the hadronic tensor $W_{\mu\nu}$, and it does not contribute to the Drell-Yan angular distribution. The sum or difference of our unpolarized and polarized contributions corresponds to the contributions from initial-state partons of the same or different fixed helicity state.

Equation (C1) in Appendix C shows that the polarized quark-antiquark contributions to the helicity structure functions are the same as the unpolarized contributions,

$$\begin{aligned} \Delta w_T^{q\bar{q}} &= w_T^{q\bar{q}}, \qquad \Delta w_L^{q\bar{q}} = w_L^{q\bar{q}}, \\ \Delta w_{\Delta\Delta}^{q\bar{q}} &= w_{\Delta\Delta}^{q\bar{q}}, \qquad \Delta w_{\Delta}^{q\bar{q}} = w_{\Delta}^{q\bar{q}}, \end{aligned} \tag{19}$$

with all unpolarized contributions given in Eq. (14).

In treating quark-gluon scattering, we present results separately for the quark-gluon and gluon-quark initial states. Equation (C5) in Appendix C provides the contribution from the quark-gluon scattering subprocess with polarized initial states:

$$\begin{aligned} \Delta w_T^{qg} &= e_q^2 \frac{8\pi^2\alpha_s}{3}\left(\frac{Q^2}{Q_\perp^2}\right)\left[1 - z_2\sqrt{1+Q_\perp^2/Q^2}\right] T_R\left[[z_2^2 - (z_1z_2 - 1)^2] + \frac{1}{2}\frac{Q_\perp^2}{Q^2}[z_2^2 + (z_1+z_2)^2]\right]\frac{S}{z_1z_2}\delta(\hat{s}+\hat{t}+\hat{u}-Q^2), \\ \Delta w_L^{qg} &= e_q^2 \frac{8\pi^2\alpha_s}{3}\left[1 - z_2\sqrt{1+Q_\perp^2/Q^2}\right] T_R[z_2^2 - (z_1+z_2)^2]\frac{S}{z_1z_2}\delta(\hat{s}+\hat{t}+\hat{u}-Q^2), \\ \Delta w_{\Delta\Delta}^{qg} &= e_q^2 \frac{8\pi^2\alpha_s}{3}\left[1 - z_2\sqrt{1+Q_\perp^2/Q^2}\right] \frac{1}{2} T_R[z_2^2 - (z_1+z_2)^2]\frac{S}{z_1z_2}\delta(\hat{s}+\hat{t}+\hat{u}-Q^2) = \frac{1}{2}\Delta w_L^{qg}, \\ \Delta w_{\Delta}^{qg} &= e_q^2 \frac{8\pi^2\alpha_s}{3}\left(\frac{Q}{Q_\perp}\right)\left[1 - z_2\sqrt{1+Q_\perp^2/Q^2}\right] T_R[-z_1^2]\frac{S}{z_1z_2}\delta(\hat{s}+\hat{t}+\hat{u}-Q^2). \end{aligned} \tag{20}$$

As shown in Eq. (C8) of Appendix C, the contribution from the gluon-quark scattering subprocess with polarized initial states is

$$\begin{aligned} \Delta w_T^{gq} &= e_q^2 \frac{8\pi^2\alpha_s}{3}\left(\frac{Q^2}{Q_\perp^2}\right)\left[1 - z_1\sqrt{1+Q_\perp^2/Q^2}\right] T_R\left[[z_1^2 - (z_1z_2 - 1)^2] + \frac{1}{2}\frac{Q_\perp^2}{Q^2}[z_1^2 + (z_1+z_2)^2]\right]\frac{S}{z_1z_2}\delta(\hat{s}+\hat{t}+\hat{u}-Q^2), \\ \Delta w_L^{gq} &= e_q^2 \frac{8\pi^2\alpha_s}{3}\left[1 - z_1\sqrt{1+Q_\perp^2/Q^2}\right] T_R[z_1^2 - (z_1+z_2)^2]\frac{S}{z_1z_2}\delta(\hat{s}+\hat{t}+\hat{u}-Q^2), \\ \Delta w_{\Delta\Delta}^{gq} &= e_q^2 \frac{8\pi^2\alpha_s}{3}\left[1 - z_1\sqrt{1+Q_\perp^2/Q^2}\right] \frac{1}{2} T_R[z_1^2 - (z_1+z_2)^2]\frac{S}{z_1z_2}\delta(\hat{s}+\hat{t}+\hat{u}-Q^2) = \frac{1}{2}\Delta w_L^{gq}, \\ \Delta w_{\Delta}^{gq} &= e_q^2 \frac{8\pi^2\alpha_s}{3}\left(\frac{Q}{Q_\perp}\right)\left[1 - z_1\sqrt{1+Q_\perp^2/Q^2}\right] T_R[z_2^2]\frac{S}{z_1z_2}\delta(\hat{s}+\hat{t}+\hat{u}-Q^2). \end{aligned} \tag{21}$$

We note that, other than for Δw_Δ^{gq}, the contributions from the gluon-quark subprocess are effectively the same as those from the quark-gluon subprocess, with z_1 and z_2 switched.

C. Limit of $Q_\perp/Q \to 0$

In this subsection, we examine the analytic behavior of each parton-level helicity structure function as $Q_\perp/Q \to 0$. Keeping up to the leading power terms, we can simplify the parton-level Mandelstam variables and the phase space δ function as

$$\begin{aligned} \hat{s} &\Rightarrow \frac{Q_\perp^2}{(1-z_1)(1-z_2)}, \qquad \hat{t} \Rightarrow -\frac{Q_\perp^2}{(1-z_2)}, \\ \hat{u} &\Rightarrow -\frac{Q_\perp^2}{(1-z_1)}. \end{aligned} \tag{22}$$

The expression for $\hat{s}$ is an immediate consequence of the phase space δ function, which, in turn, can be expanded as [29]

$$\frac{S}{z_1z_2}\delta(\hat{s}+\hat{t}+\hat{u}-Q^2) \Rightarrow \frac{1}{x_1x_2}\left[\frac{\delta(1-z_2)}{(1-z_1)_+} + \frac{\delta(1-z_1)}{(1-z_2)_+} + \delta(1-z_1)\delta(1-z_2)\ln\frac{Q^2}{Q_\perp^2}\right]. \tag{23}$$

The standard definition of "+" distribution is

$$\int_x^1 dz \frac{f(z)}{(1-z)_+} = \int_x^1 dz \frac{f(z)-f(1)}{(1-z)} + f(1)\ln(1-x). \tag{24}$$

Substituting Eqs. (22) and (23) into Eqs. (14) and (16), we obtain the analytic behavior of the perturbatively calculated parton-level helicity structure functions as $Q_\perp/Q \to 0$. For the quark-antiquark annihilation process, these are

$$
\begin{aligned}
w_T^{q\bar{q}} &\Rightarrow e_q^2 \frac{8\pi^2\alpha_s}{3x_1x_2}\left(\frac{Q^2}{Q_\perp^2}\right)\left\{P_{qq}(z_2)\delta(1-z_1)+P_{qq}(z_1)\delta(1-z_2)+2C_F\delta(1-z_1)\delta(1-z_2)\left[\ln\left(\frac{Q^2}{Q_\perp^2}\right)-\frac{3}{2}\right]\right\},\\
w_L^{q\bar{q}} &\Rightarrow e_q^2 \frac{8\pi^2\alpha_s}{3x_1x_2}\left\{P_{qq}(z_2)\delta(1-z_1)+P_{qq}(z_1)\delta(1-z_2)+2C_F\delta(1-z_1)\delta(1-z_2)\left[\ln\left(\frac{Q^2}{Q_\perp^2}\right)-\frac{3}{2}\right]\right\},\\
w_{\Delta\Delta}^{q\bar{q}} &\Rightarrow \frac{1}{2}e_q^2 \frac{8\pi^2\alpha_s}{3x_1x_2}\left\{P_{qq}(z_2)\delta(1-z_1)+P_{qq}(z_1)\delta(1-z_2)+2C_F\delta(1-z_1)\delta(1-z_2)\left[\ln\left(\frac{Q^2}{Q_\perp^2}\right)-\frac{3}{2}\right]\right\},\\
w_{\Delta}^{q\bar{q}} &\Rightarrow e_q^2 \frac{8\pi^2\alpha_s}{3x_1x_2}\left(\frac{Q}{Q_\perp}\right)\{C_F[1+z_2]\delta(1-z_1)-C_F[1+z_1]\delta(1-z_2)\}.
\end{aligned}
\tag{25}
$$

For the quark-gluon subprocess, the small $Q_\perp$ behavior is

$$
\begin{aligned}
w_T^{qg} &\Rightarrow e_q^2 \frac{8\pi^2\alpha_s}{3x_1x_2}\left(\frac{Q^2}{Q_\perp^2}\right)P_{qg}(z_2)\delta(1-z_1),\\
w_L^{qg} &\Rightarrow e_q^2 \frac{8\pi^2\alpha_s}{3x_1x_2}P_{qg}(-z_2)\delta(1-z_1),\\
w_{\Delta\Delta}^{qg} &\Rightarrow \frac{1}{2}e_q^2 \frac{8\pi^2\alpha_s}{3x_1x_2}P_{qg}(-z_2)\delta(1-z_1),\\
w_{\Delta}^{qg} &\Rightarrow e_q^2 \frac{8\pi^2\alpha_s}{3x_1x_2}\left(\frac{Q}{Q_\perp}\right)T_R[1-2z_2^2]\delta(1-z_1).
\end{aligned}
\tag{26}
$$

The parton-to-parton splitting functions are

$$
P_{qq}(z) = C_F\left[\frac{1+z^2}{(1-z)_+}+\frac{3}{2}\delta(1-z)\right], \tag{27}
$$

$$
P_{qg}(z) = T_R[z^2+(1-z)^2]. \tag{28}
$$

With z_1 and z_2 switched, Eq. (26) is also true for the gluon-quark subprocess, except for w_Δ^{gq} which needs an extra overall minus sign. Our results for the form of the helicity structure functions for unpolarized incoming partons as $Q_\perp/Q \to 0$ in Eqs. (25) and (26) are consistent with those derived in Ref. [11].

Equation (19) allows us to conclude that, at this order, the analytic behavior of the quark-antiquark annihilation subprocess as $Q_\perp/Q \to 0$ is independent of whether incoming (anti)quarks are spin averaged or polarized. The contributions to the parton-level helicity structure functions are given in Eq. (25).

On the other hand, the polarized contributions from the quark-gluon scattering subprocess are different from those for "spin-averaged" initial parton states. From Eq. (20), we obtain

$$
\begin{aligned}
\Delta w_T^{qg} &\Rightarrow e_q^2 \frac{8\pi^2\alpha_s}{3x_1x_2}\left(\frac{Q^2}{Q_\perp^2}\right)\Delta P_{qg}(z_2)\delta(1-z_1),\\
\Delta w_L^{qg} &\Rightarrow e_q^2 \frac{8\pi^2\alpha_s}{3x_1x_2}\Delta P_{qg}(-z_2)\delta(1-z_1),\\
\Delta w_{\Delta\Delta}^{qg} &\Rightarrow \frac{1}{2}e_q^2 \frac{8\pi^2\alpha_s}{3x_1x_2}\Delta P_{qg}(-z_2)\delta(1-z_1),\\
\Delta w_{\Delta}^{qg} &\Rightarrow e_q^2 \frac{8\pi^2\alpha_s}{3x_1x_2}\left(\frac{Q}{Q_\perp}\right)[-T_R\delta(1-z_1)],
\end{aligned}
\tag{29}
$$

where $\Delta P_{qg}(z)$ is the leading polarized gluon-to-quark splitting function

$$
\Delta P_{qg}(z) = T_R[z^2-(1-z)^2]. \tag{30}
$$

Similarly, based on Eq. (21), the small $Q_\perp$ behavior of the polarized gluon-quark contribution is

$$
\begin{aligned}
\Delta w_T^{gq} &\Rightarrow e_q^2 \frac{8\pi^2\alpha_s}{3x_1x_2}\left(\frac{Q^2}{Q_\perp^2}\right)\Delta P_{qg}(z_1)\delta(1-z_2),\\
\Delta w_L^{gq} &\Rightarrow e_q^2 \frac{8\pi^2\alpha_s}{3x_1x_2}\Delta P_{qg}(-z_1)\delta(1-z_2),\\
\Delta w_{\Delta\Delta}^{gq} &\Rightarrow \frac{1}{2}e_q^2 \frac{8\pi^2\alpha_s}{3x_1x_2}\Delta P_{qg}(-z_1)\delta(1-z_2),\\
\Delta w_{\Delta}^{gq} &\Rightarrow e_q^2 \frac{8\pi^2\alpha_s}{3x_1x_2}\left(\frac{Q}{Q_\perp}\right)[T_R\delta(1-z_2)].
\end{aligned}
\tag{31}
$$

Clearly, the perturbatively calculated helicity structure functions at order of α_s and beyond are singular as $Q_\perp/Q \to 0$: W_T and W_Δ have the power divergences, $Q^2/Q_\perp^2$ and $Q/Q_\perp$, respectively, as well as $\ln(Q/Q_\perp)$ divergences, whereas W_L and $W_{\Delta\Delta}$ show $\ln(Q/Q_\perp)$ divergences [10,11,13,14].

III. ASYMPTOTIC CURRENT-CONSERVING TENSOR

In this section, we investigate the possible connection between the logarithmic divergences of different helicity structure functions, and we show that they have a common origin. We observe that the four helicity structure functions cannot be independent as $Q_\perp = 0$ where the general tensor decomposition in the virtual photon rest frame in Eq. (4) is ill defined. We construct a new asymptotic hadronic tensor

that has the right number of independent scalar functions as $Q_\perp \to 0$ by requiring that the singular contribution to the hadronic tensor should satisfy electromagnetic current conservation to all orders in α_s. We show explicitly that the $Q_\perp/Q \to 0$ singular contributions in W_T, W_L, and $W_{\Delta\Delta}$ are related uniquely to the singular contribution of the angular-integrated cross section.

The general arguments in Ref. [26] show that there should be only two independent power-divergent scalar functions as $Q_\perp/Q \to 0$ in the Collins-Soper frame. To display the explicit dependence of the hadronic tensor on $Q_\perp/Q$, we rewrite the unit vectors of the Collins-Soper frame in Eq. (5) as

$$\begin{aligned} T^\mu &= \frac{1}{\sqrt{2}}\sqrt{1+\frac{Q_\perp^2}{Q^2}}[e^y\bar{n}^\mu + e^{-y}n^\mu] + \left(\frac{Q_\perp}{Q}\right)n_\perp^\mu, \\ Z^\mu &= \frac{1}{\sqrt{2}}[e^y\bar{n}^\mu - e^{-y}n^\mu], \\ X^\mu &= \frac{1}{\sqrt{2}}\left(\frac{Q_\perp}{Q}\right)[e^y\bar{n}^\mu + e^{-y}n^\mu] + \sqrt{1+\frac{Q_\perp^2}{Q^2}}n_\perp^\mu, \end{aligned} \tag{32}$$

with Y^μ uniquely fixed. By expanding the full Drell-Yan hadronic tensor in Eq. (4) and using Eq. (32) in the limit $Q_\perp/Q \to 0$, we obtain the following form for the singular terms of the tensor [27,30]:

$$\begin{aligned} W_{\rm Sing}^{\mu\nu} &= (-g^{\mu\nu} + \bar{n}^\mu n^\nu + n^\mu\bar{n}^\nu)W_2^{\rm Asym} \\ &\quad + \frac{1}{\sqrt{2}}\left[\frac{Q_\perp}{Q}(n_\perp^\mu\bar{n}^\nu + \bar{n}^\mu n_\perp^\nu)e^y\right] \\ &\quad \times \left(W_2^{\rm Asym} - \frac{Q}{Q_\perp}W_1^{\rm Asym}\right) \\ &\quad + \frac{1}{\sqrt{2}}\left[\frac{Q_\perp}{Q}(n_\perp^\mu n^\nu + n^\mu n_\perp^\nu)e^{-y}\right] \\ &\quad \times \left(W_2^{\rm Asym} + \frac{Q}{Q_\perp}W_1^{\rm Asym}\right). \end{aligned} \tag{33}$$

At this point, there are two unspecified divergent scalar functions: $W_2^{\rm Asym} \propto Q^2/Q_\perp^2$ and $W_1^{\rm Asym} \propto Q/Q_\perp$ as $Q_\perp/Q \to 0$. In Eq. (33), the unit vectors $\bar{n}$, n, $n_\perp$ specify the center-of-mass frame of the hadron collision, defined in Appendix A.

The singular tensor as $Q_\perp/Q \to 0$ in Eq. (33) is not current conserving since $q_\mu W_{\rm Sing}^{\mu\nu} \neq 0$. In order to resum the singular terms of the hadronic tensor to all orders in α_s, we require a tensor that incorporates all the singular terms *and* also conserves the current perturbatively at any order of α_s. We use the term *asymptotic tensor* for this current-conserving tensor. We define it to be

$$\begin{aligned} W_{\rm Asym}^{\mu\nu} &= (-g^{\mu\nu} + \bar{n}^\mu n^\nu + n^\mu\bar{n}^\nu)W_2^{\rm Asym} \\ &\quad + \frac{Q_\perp}{Q^-}\left(n_\perp^\mu\bar{n}^\nu + \bar{n}^\mu n_\perp^\nu + \frac{Q_\perp}{Q^-}\bar{n}^\mu\bar{n}^\nu\right) \\ &\quad \times \frac{1}{2}\left[W_2^{\rm Asym} - \frac{Q}{Q_\perp}W_1^{\rm Asym}\right] \\ &\quad + \frac{Q_\perp}{Q^+}\left(n_\perp^\mu n^\nu + n^\mu n_\perp^\nu + \frac{Q_\perp}{Q^+}n^\mu n^\nu\right) \\ &\quad \times \frac{1}{2}\left[W_2^{\rm Asym} + \frac{Q}{Q_\perp}W_1^{\rm Asym}\right], \end{aligned} \tag{34}$$

where the components of the virtual photon momentum $Q^+ = q\cdot n$ and $Q^- = q\cdot\bar{n}$ are defined in Appendix A. The asymptotic tensor in Eq. (34) is equal to the singular tensor in Eq. (33) plus a minimal nonsingular term such that $q_\mu W_{\rm Asym}^{\mu\nu} = 0$.

The angular-integrated cross section is obtained from the trace, $d\sigma/d^4q \propto -g_{\mu\nu}W^{\mu\nu}$. The trace of the asymptotic tensor in Eq. (34) should therefore be fixed by the asymptotic term $W^{\rm Asym}$ of the angular-integrated Drell-Yan transverse momentum distribution [25]. This statement allows us to fix uniquely the asymptotically divergent function $W_2^{\rm Asym}$ in Eq. (34). We obtain

$$W_2^{\rm Asym} = W^{\rm Asym}/2. \tag{35}$$

The angular-integrated cross section fixes the value of $W_2^{\rm Asym}$, but it cannot fix the second scalar function $W_1^{\rm Asym}$ in Eq. (34). This second function represents the singular perturbative behavior of the structure function W_Δ. We defer discussion of W_Δ until Sec. V and concentrate on transverse momentum resummation for the other three helicity structure functions, W_T, W_L, and $W_{\Delta\Delta}$.

We reexpress the asymptotic tensor in terms of the previously defined unit vectors in the Collins-Soper frame as

$$\begin{aligned} W_{\rm Asym}^{\mu\nu} &= \left[(-g^{\mu\nu} + T^\mu T^\nu) - \frac{Q_\perp^2/Q^2}{1+Q_\perp^2/Q^2}X^\mu X^\nu \right. \\ &\quad \left. - \frac{1}{1+Q_\perp^2/Q^2}Z^\mu Z^\nu\right]\frac{W^{\rm Asym}}{2} \\ &\quad - \frac{1}{1+Q_\perp^2/Q^2}[X^\mu Z^\nu + Z^\mu X^\nu]W_1^{\rm Asym}. \end{aligned} \tag{36}$$

Upon comparison with Eq. (4), we immediately derive the corresponding asymptotic helicity structure functions,

$$W_T^{\mathrm{Asym}} = \left(1 - \frac{1}{2}\frac{Q_\perp^2/Q^2}{1+Q_\perp^2/Q^2}\right)\frac{W^{\mathrm{Asym}}}{2} \approx \frac{W^{\mathrm{Asym}}}{2},$$
$$W_L^{\mathrm{Asym}} = \frac{Q_\perp^2/Q^2}{1+Q_\perp^2/Q^2}\frac{W^{\mathrm{Asym}}}{2} \approx \frac{Q_\perp^2}{Q^2}\frac{W^{\mathrm{Asym}}}{2}, \qquad (37)$$
$$W_{\Delta\Delta}^{\mathrm{Asym}} = \frac{1}{2}\frac{Q_\perp^2/Q^2}{1+Q_\perp^2/Q^2}\frac{W^{\mathrm{Asym}}}{2} \approx \frac{1}{2}\frac{Q_\perp^2}{Q^2}\frac{W^{\mathrm{Asym}}}{2}.$$

Equation (37) shows that current conservation relates the $Q_\perp/Q \to 0$ divergent terms of the transverse, longitudinal, and double spin-flip structure functions intimately to the divergent part of the angular-integrated transverse momentum distribution. The next key question, addressed affirmatively in the next section, is whether the asymptotic helicity structure functions in Eq. (37), as derived here, are sufficient to remove all the leading divergences in the perturbatively calculated structure functions order by order in α_s.

IV. PERTURBATIVE FINITE TENSOR

We show in this section that the three asymptotic helicity structure functions presented in the last section include all the $Q_\perp/Q \to 0$ leading divergent terms of the corresponding perturbatively calculated helicity structure functions, and therefore, that we can define a perturbatively finite tensor from the difference,

$$W_{\mathrm{Finite}}^{\mu\nu} \equiv W_{\mathrm{Pert}}^{\mu\nu} - W_{\mathrm{Asym}}^{\mu\nu}, \qquad (38)$$

at any order of α_s. This finite tensor conserves the current since the asymptotic tensor conserves the current.

The $Q_\perp/Q \to 0$ divergent part of the angular-integrated cross section is obtained from the trace of the hadronic tensor $g_{\mu\nu}W^{\mu\nu}$. Applying this statement at the parton level, we use the results of Sec. III to derive the $Q_\perp/Q \to 0$ asymptotic terms for the angular-integrated and spin-averaged $q\bar{q} \to \gamma^* g$ and $qg \to \gamma^* q$ subprocesses. These are

$$\frac{w_{q\bar{q}}^{\mathrm{Asym}}}{2} \approx e_q^2 \frac{8\pi^2\alpha_s}{3x_1x_2}\frac{Q^2}{Q_\perp^2}\Big\{P_{qq}(z_2)\delta(1-z_1) + P_{qq}(z_1)\delta(1-z_2) + 2C_F\delta(1-z_1) \times \delta(1-z_2)\Big[\ln\Big(\frac{Q^2}{Q_\perp^2}\Big) - \frac{3}{2}\Big]\Big\};$$
$$\frac{w_{qg}^{\mathrm{Asym}}}{2} \approx e_q^2 \frac{8\pi^2\alpha_s}{3x_1x_2}\frac{Q^2}{Q_\perp^2}P_{qg}(z_2)\delta(1-z_1);$$
$$\frac{w_{gq}^{\mathrm{Asym}}}{2} \approx e_q^2 \frac{8\pi^2\alpha_s}{3x_1x_2}\frac{Q^2}{Q_\perp^2}P_{qg}(z_1)\delta(1-z_2). \qquad (39)$$

Using Eq. (37) at the parton level, we find that as $Q_\perp/Q \to 0$, the parton-level asymptotic terms in Eq. (39) remove all divergent contributions of the corresponding perturbatively calculated helicity structure functions. For the quark-antiquark annihilation subprocess,

$$w_T^{q\bar{q}} - \left(1 - \frac{1}{2}\frac{Q_\perp^2/Q^2}{1+Q_\perp^2/Q^2}\right)\frac{w_{q\bar{q}}^{\mathrm{Asym}}}{2} \Rightarrow \mathcal{O}(Q_\perp^0),$$
$$w_L^{q\bar{q}} - \frac{Q_\perp^2/Q^2}{1+Q_\perp^2/Q^2}\frac{w_{q\bar{q}}^{\mathrm{Asym}}}{2} \Rightarrow \mathcal{O}(Q_\perp^2), \qquad (40)$$
$$w_{\Delta\Delta}^{q\bar{q}} - \frac{1}{2}\frac{Q_\perp^2/Q^2}{1+Q_\perp^2/Q^2}\frac{w_{q\bar{q}}^{\mathrm{Asym}}}{2} \Rightarrow \mathcal{O}(Q_\perp^2).$$

For the quark-gluon subprocess,

$$w_T^{qg} - \left(1 - \frac{1}{2}\frac{Q_\perp^2/Q^2}{1+Q_\perp^2/Q^2}\right)\frac{w_{qg}^{\mathrm{Asym}}}{2} \Rightarrow \mathcal{O}(Q_\perp^0),$$
$$w_L^{qg} - \frac{Q_\perp^2/Q^2}{1+Q_\perp^2/Q^2}\frac{w_{qg}^{\mathrm{Asym}}}{2} \Rightarrow e_q^2\frac{8\pi^2\alpha_s}{3x_1x_2}\delta(1-z_1)[P_{qg}(-z_2) - P_{qg}(z_2)] + \mathcal{O}(Q_\perp^2), \qquad (41)$$
$$w_{\Delta\Delta}^{qg} - \frac{1}{2}\frac{Q_\perp^2/Q^2}{1+Q_\perp^2/Q^2}\frac{w_{qg}^{\mathrm{Asym}}}{2} \Rightarrow \frac{1}{2}e_q^2\frac{8\pi^2\alpha_s}{3x_1x_2}\delta(1-z_1)[P_{qg}(-z_2) - P_{qg}(z_2)] + \mathcal{O}(Q_\perp^2).$$

With z_1 and z_2 interchanged, Eq. (41) is also true for the gluon-quark subprocess. Other than the nonlogarithmic finite piece (as $Q_\perp/Q \to 0$) in the quark-gluon contributions to W_L and $W_{\Delta\Delta}$, the asymptotic tensor completely removes the leading term of the perturbatively calculated helicity structure functions as $Q_\perp/Q \to 0$.

The parton-level asymptotic terms for the polarized quark-antiquark, quark-gluon, and gluon-quark subprocesses are

$$\frac{\Delta w_{q\bar{q}}^{\mathrm{Asym}}}{2} \approx \frac{w_{q\bar{q}}^{\mathrm{Asym}}}{2},$$
$$\frac{\Delta w_{qg}^{\mathrm{Asym}}}{2} \approx e_q^2\frac{8\pi^2\alpha_s}{3x_1x_2}\frac{Q^2}{Q_\perp^2}\Delta P_{qg}(z_2)\delta(1-z_1), \qquad (42)$$
$$\frac{\Delta w_{gq}^{\mathrm{Asym}}}{2} \approx e_q^2\frac{8\pi^2\alpha_s}{3x_1x_2}\frac{Q^2}{Q_\perp^2}\Delta P_{qg}(z_1)\delta(1-z_2).$$

Since $\Delta\omega^{\mu\nu}_{q\bar{q}} = \omega^{\mu\nu}_{q\bar{q}}$, and $\Delta w^{\rm Asym}_{q\bar{q}} = w^{\rm Asym}_{q\bar{q}}$, Eq. (40) is true also for the polarized quark-antiquark subprocess.

The finite contributions in the parton-level helicity structure functions for polarized quark-gluon or gluon-quark subprocesses are not the same as those for the corresponding unpolarized subprocesses. We find

$$\begin{aligned}
\Delta w^{qg}_T - \left(1 - \frac{1}{2}\frac{Q^2_\perp/Q^2}{1+Q^2_\perp/Q^2}\right)\frac{\Delta w^{\rm Asym}_{qg}}{2} &\Rightarrow \mathcal{O}(Q^0_\perp),\\
\Delta w^{qg}_L - \frac{Q^2_\perp/Q^2}{1+Q^2_\perp/Q^2}\frac{\Delta w^{\rm Asym}_{qg}}{2} &\Rightarrow e_q^2\frac{8\pi^2\alpha_s}{3x_1x_2}\delta(1-z_1)[\Delta P_{qg}(-z_2) - \Delta P_{qg}(z_2)] + \mathcal{O}(Q^2_\perp),\\
\Delta w^{qg}_{\Delta\Delta} - \frac{1}{2}\frac{Q^2_\perp/Q^2}{1+Q^2_\perp/Q^2}\frac{\Delta w^{\rm Asym}_{qg}}{2} &\Rightarrow \frac{1}{2}e_q^2\frac{8\pi^2\alpha_s}{3x_1x_2}\delta(1-z_1)[\Delta P_{qg}(-z_2) - \Delta P_{qg}(z_2)] + \mathcal{O}(Q^2_\perp).
\end{aligned} \tag{43}$$

With z_1 and z_2 interchanged, Eq. (43) is also true for the gluon-quark subprocess.

The uncanceled finite term in the helicity structure functions W_L and $W_{\Delta\Delta}$ is proportional to

$$P_{qg}(-z_2) - P_{qg}(z_2) = 4z_2T_R, \tag{44}$$

for unpolarized initial partonic states, and to

$$\Delta P_{qg}(-z_2) - \Delta P_{qg}(z_2) = -4z_2T_R, \tag{45}$$

for the polarized initial partonic states. Therefore, for the scattering of two polarized hadrons with the same helicity (both positive or negative), the quark-gluon contribution to the perturbatively finite term of the helicity structure functions W_L and $W_{\Delta\Delta}$ vanishes as $Q_\perp/Q \to 0$. This result is obtained because the perturbative contribution to the longitudinal and double spin-flip helicity structure functions is proportional to $P_{qg}(-z_2) + \Delta P_{qg}(-z_2)$ in the limit of $Q_\perp/Q \to 0$, the corresponding asymptotic term is proportional to $P_{qg}(z_2) + \Delta P_{qg}(z_2)$, and the difference vanishes due to Eqs. (44) and (45). We also observe that, at this order, the uncanceled term in the quark-gluon subprocess is proportional to the helicity flipping splitting function,

$$P_{q^-g^+}(z) = P_{q^+g^-}(z) = T_R(1-z)^2. \tag{46}$$

The finite term as $Q_\perp/Q \to 0$ for the quark-antiquark subprocess at this order is removed completely by the asymptotic term since the helicity flipping splitting function for the quark vanishes at this order, $P_{q^-q^+}(z) = P_{q^+q^-}(z) = 0$.

Our observations allow us to claim that transverse momentum dependent factorization for the full hadronic tensor, which is the basis for the Collins-Soper-Sterman b-space resummation, breaks at subleading power in the $Q_\perp/Q$ expansion, but only in the helicity flipping channel. The breaking seems not to supply leading logarithmic terms.

The asymptotic current-conserving tensor introduced in the last section is sufficient to remove all leading divergent terms in the perturbatively calculated hadronic tensor. The logarithmic terms in the perturbatively calculated helicity structure functions, W_T, W_L, and $W_{\Delta\Delta}$, are shown here to have the same origin as those in the angular-integrated cross section. Therefore, for these helicity structure functions we can obtain a perturbatively finite difference as

$$W_i^{\rm Finite} \equiv W_i^{\rm Pert} - W_i^{\rm Asym}, \tag{47}$$

with $i = T, L, \Delta\Delta$.

V. FULL HADRONIC TENSOR INCLUDING TRANSVERSE MOMENTUM RESUMMATION

In this section we present expressions for the transverse momentum dependence of the structure functions incorporating resummation to all orders in α_s of the singular divergent behavior as $Q_\perp/Q \to 0$ and including the contributions at order α_s that are finite in the small $Q_\perp$ limit. We begin first with a brief summary of the resummation formalism developed for the angular-integrated cross section.

As explained above, when $Q_\perp \ll Q$, the $Q_\perp$ distribution of the helicity structure functions calculated in conventional fixed-order perturbation theory receives a large logarithmic term, $\ln(Q/Q_\perp)$, at every power of α_s, which is a direct consequence of the emission of soft and collinear gluons from the incident partons. Therefore, when $Q_\perp/Q$ is sufficiently small, the convergence of the conventional perturbative expansion in powers of α_s is impaired, and the logarithmic terms must be resummed.

Resummation of the large logarithmic terms can be carried out either in $Q_\perp$ space directly, or in the impact parameter, b space, which is the Fourier conjugate of $Q_\perp$ space. It was first shown by Dokshitzer, Diakonov, and Troian that, in the double leading logarithm approximation, the dominant contributions in the small Q_T region can be resummed into a Sudakov form factor [22]. By imposing transverse momentum conservation without assuming strong ordering in the transverse momenta of radiated gluons, Parisi and Petronzio introduced a b-space resummation method which allows one to resum some subleading logarithmic terms [23]. Using a renormalization group equation technique, Collins and Soper improved b-space resummation to resum all terms as singular as $\ln^m(Q^2/Q^2_\perp)/Q^2_\perp$, as $Q_\perp \to 0$ [24]. Using this renormal-

ization group improved b-space resummation, Collins, Soper, and Sterman (CSS) derived a formalism for the transverse momentum distributions of vector boson production in hadronic collisions [25]. This CSS formalism, developed originally for angular-integrated vector boson production, casts the cross section in the following generic form [25]:

$$\frac{d\sigma}{d^4q} = \frac{1}{(2\pi)^2}\int d^2b e^{i\vec{Q}_\perp\cdot\vec{b}}\tilde{W}(b, Q, x_1, x_2) + Y(Q_\perp, Q, x_1, x_2). \tag{48}$$

The function $\tilde{W}$ provides the dominant contribution when $Q_\perp \ll Q$, while the Y term supplies contributions that are negligible for small $Q_\perp$ but become important, in practice, when $Q_\perp \sim Q$. The function $\tilde{W}$ in Eq. (48) incorporates all powers of large logarithmic contributions from $\ln(1/b^2)$ to $\ln(Q^2)$. It has the following form [25]:

$$\tilde{W}(b, Q, x_1, x_2) = \mathrm{e}^{-S(b,Q)}\tilde{W}(b, c/b, x_1, x_2), \tag{49}$$

where c is a constant of order 1 [25], and

$$S(b, Q) = \int_{c^2/b^2}^{Q^2}\frac{d\mu^2}{\mu^2}\left[\ln\left(\frac{Q^2}{\mu^2}\right)A(\alpha_s(\mu)) + B(\alpha_s(\mu))\right]. \tag{50}$$

Functions $A(\alpha_s)$ and $B(\alpha_s)$ may be calculated perturbatively in powers of α_s [25]. Function $\tilde{W}(b, c/b, x_A, x_B)$ in Eq. (49) depends only on one momentum scale, $1/b$, and it may be calculated perturbatively as long as $1/b$ is large enough. The large logarithms from $\ln(c^2/b^2)$ to $\ln(Q^2)$ in $\tilde{W}(b, Q, x_1, x_2)$ are completely resummed into the exponential factor $\exp[-S(b, Q)]$. The finite Y term is defined to be the difference between the cross section calculated in conventional fixed-order perturbation theory and the asymptotic cross section which is equal to the perturbative expansion of the resummed part of the cross section, the first term on the RHS of Eq. (48).

The function $\tilde{W}(b, Q, x_1, x_2)$ of the CSS b-space resummation formalism in Eq. (48) is not exactly equal to the Fourier transform of the transverse momentum distribution, but its Fourier transform reproduces all leading divergences of the type $\ln^m(Q^2/Q_\perp^2)/Q_\perp^2$ in the perturbatively calculated transverse momentum spectrum when $Q_\perp/Q \to 0$. Combined with the perturbatively finite Y term, the Fourier transform of the resummed $\tilde{W}(b, Q, x_1, x_2)$ gives a good description of heavy vector boson production at collider energies [31,32].

The transverse momentum dependence of the angular distribution of leptons from the Drell-Yan mechanism is determined by the transverse momentum dependence of the helicity structure functions. Only the transverse structure function W_T has a leading divergence of the type $\ln^m(Q^2/Q_\perp^2)/Q_\perp^2$ as $Q_\perp/Q \to 0$. It might be natural to consider the resummation of these large logarithms into W_T [10,13,14]. However, as we demonstrate in Eqs. (34) and (36), electromagnetic current conservation requires that the leading logarithmic divergences of the structure functions W_L and $W_{\Delta\Delta}$ share the same origin as those in W_T and those in the angular-integrated cross section. All are included in one asymptotic function, W^{Asym}. Resummation of the large logarithmic terms of the Drell-Yan helicity structure functions can therefore be accomplished in terms of the resummed contribution to the angular-integrated Drell-Yan cross section. Referring to Eq. (37), we obtain the resummed contribution to the helicity structure functions in the Collins-Soper frame as

$$\begin{aligned} W_T^{\mathrm{Resum}} &= \left(1 - \frac{1}{2}\frac{Q_\perp^2/Q^2}{1 + Q_\perp^2/Q^2}\right)\frac{W^{\mathrm{Resum}}}{2}, \\ W_L^{\mathrm{Resum}} &= \frac{Q_\perp^2/Q^2}{1 + Q_\perp^2/Q^2}\frac{W^{\mathrm{Resum}}}{2}, \\ W_{\Delta\Delta}^{\mathrm{Resum}} &= \frac{1}{2}\frac{Q_\perp^2/Q^2}{1 + Q_\perp^2/Q^2}\frac{W^{\mathrm{Resum}}}{2}. \end{aligned} \tag{51}$$

All depend on the same QCD resummed expression W^{Resum} that pertains to the angular-integrated Drell-Yan cross section [25]. By comparing Eq. (48) with Eq. (2), we obtain

$$\frac{\alpha_{\mathrm{em}}^2}{12\pi^3 S^2 Q^2}W^{\mathrm{Resum}} = \frac{1}{(2\pi)^2}\int d^2b e^{i\vec{Q}_\perp\cdot\vec{b}}\tilde{W}(b, Q, x_1, x_2). \tag{52}$$

In analogy to the CSS result for the angular-integrated cross section in Eq. (48), the expressions for the full transverse momentum distribution of the helicity structure functions are

$$\begin{aligned} W_T &= \left(1 - \frac{1}{2}\frac{Q_\perp^2/Q^2}{1 + Q_\perp^2/Q^2}\right)\frac{W^{\mathrm{Resum}}}{2} + \left[W_T^{\mathrm{Pert}} - \left(1 - \frac{1}{2}\frac{Q_\perp^2/Q^2}{1 + Q_\perp^2/Q^2}\right)\frac{W^{\mathrm{Asym}}}{2}\right], \\ W_L &= \frac{Q_\perp^2/Q^2}{1 + Q_\perp^2/Q^2}\frac{W^{\mathrm{Resum}}}{2} + \left[W_L^{\mathrm{Pert}} - \frac{Q_\perp^2/Q^2}{1 + Q_\perp^2/Q^2}\frac{W^{\mathrm{Asym}}}{2}\right], \\ W_{\Delta\Delta} &= \frac{1}{2}\frac{Q_\perp^2/Q^2}{1 + Q_\perp^2/Q^2}\frac{W^{\mathrm{Resum}}}{2} + \left[W_{\Delta\Delta}^{\mathrm{Pert}} - \frac{1}{2}\frac{Q_\perp^2/Q^2}{1 + Q_\perp^2/Q^2}\frac{W^{\mathrm{Asym}}}{2}\right] \end{aligned} \tag{53}$$

with the asymptotic term in these expressions equal to the perturbative expansion of the resummed contribution in powers of α_s. As in the case of the angular-integrated cross section, these expressions are applicable for $Q \gtrsim Q_\perp$. Other effects must be considered when $Q_\perp \gg Q$ [33–35].

Substituting the expressions for the helicity structure functions W_T and W_L from Eq. (53) into Eq. (2), we obtain

$$\frac{d\sigma}{d^4q} = \frac{\alpha_{\rm em}^2}{12\pi^3 S^2 Q^2}[W^{\rm Resum} + (2W_T^{\rm Pert} + W_L^{\rm Pert}) - W^{\rm Asym}]. \tag{54}$$

Using Eq. (48), we find that the perturbatively finite Y-term is

$$Y = \frac{\alpha_{\rm em}^2}{12\pi^3 S^2 Q^2}[(2W_T^{\rm Pert} + W_L^{\rm Pert}) - W^{\rm Asym}]. \tag{55}$$

A. Lam-Tung relation

The Lam-Tung relation states that the longitudinal and the double spin-flip structure functions obey the equality $W_L = 2W_{\Delta\Delta}$. Based on Eqs. (37) and (51) and the definition in Eq. (53), we find that possible violation of the relation can come only from the nonsingular finite piece of the perturbative contribution. The resummed contribution is known to dominate the angular-integrated cross section in the region of small and modest $Q_\perp$, and, by extension, we expect it to dominate the behavior of W_L and $W_{\Delta\Delta}$ in the same region. We conclude that violation of the Lam-Tung relation as a function of $Q_\perp$ should be relatively small, consistent with the results of perturbative calculations at order α_s^2 [9], but demonstrated here to all orders in α_s.

An alternative way to state the Lam-Tung relation is in terms of the angular coefficients λ and ν, defined in Eq. (A15). It is expressed as $1 - \lambda - 2\nu = 0$. We derive

$$\lambda = \frac{W_T - W_L}{W_T + W_L} \approx \frac{W_T^{\rm Resum} - W_L^{\rm Resum}}{W_T^{\rm Resum} + W_L^{\rm Resum}} = \frac{1 - \frac{1}{2}Q_\perp^2/Q^2}{1 + \frac{3}{2}Q_\perp^2/Q^2},$$
$$\nu = \frac{2W_{\Delta\Delta}}{W_T + W_L} \approx \frac{2W_{\Delta\Delta}^{\rm Resum}}{W_T^{\rm Resum} + W_L^{\rm Resum}} = \frac{Q_\perp^2/Q^2}{1 + \frac{3}{2}Q_\perp^2/Q^2}. \tag{56}$$

The analytic expressions in Eq. (56) were derived first in Ref. [8] based on the perturbative calculation of $q\bar{q} \to \gamma^* g$. Our result is valid for all orders in α_s if we retain only the leading resummed contribution, and it is independent of the type of incident hadrons.

A recent analysis of Fermilab data shows reasonable agreement with the Lam-Tung relation for moderate values of $Q_\perp$ [19], while early data with pion beams show some violation [15–18].

B. Phenomenological example

As an example, we show in Fig. 4 an explicit numerical evaluation of the helicity structure functions W_T and W_L computed from Eq. (53). The double spin-flip structure function $W_{\Delta\Delta} = W_L/2$ since both the resummed contributions and the finite perturbative contributions at order α_s satisfy this relationship. We choose the mass interval 8 GeV $\leq Q \leq$ 9 GeV and $E_{\rm beam} = 800$ GeV in order to compare with data from Fermilab experiment E772 [36]. The parameters we use are identical to those used for Fig. 14 in Ref. [32].

The dashed and dot-dashed lines in Fig. 4 represent the W_T and W_L contributions to the cross section, while the total contribution is proportional to $2W_T + W_L$. We remark that the transverse momentum distribution after resummation is finite as $Q_\perp \to 0$ for W_T, but it becomes vanishingly small in the case of W_L.

C. Discussion of W_Δ

As shown in Sec. III, the perturbative contribution to the single spin-flip structure function W_Δ is proportional to $Q/Q_\perp$, which is singular as $Q_\perp/Q \to 0$. Unlike the other helicity structure functions, W_Δ does not show a logarithmic divergence in the Collins-Soper frame, a feature that seems special for this frame [11]. The absence of the divergence could be a consequence of the symmetry of the frame with respect to the hadron beam directions, which requires $W_\Delta \propto \mathcal{W}_1 e^{-2y} - \mathcal{W}_2 e^{2y}$ in Eq. (A9), and the fact that the leading logarithms arise from the region of phase space where $z_1 \to 1$ and $z_2 \to 1$.

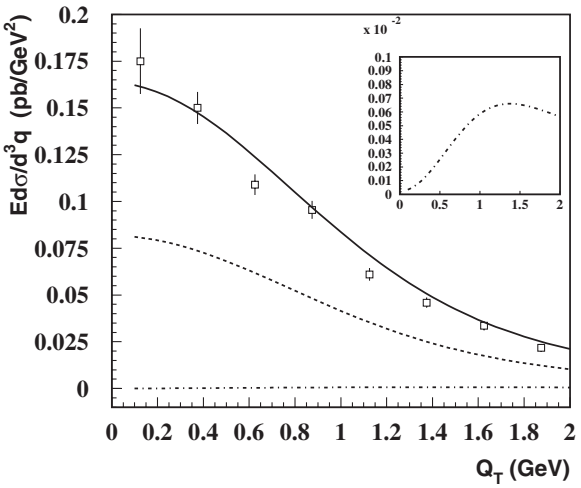

FIG. 4. The transverse momentum dependence of the angular-integrated Drell-Yan cross section, obtained from the contributions of the helicity structure functions, W_T and W_L, in Eq. (53), is shown as a solid line and compared with data from Fermilab experiment E772 [36] for Q in the interval (8,9) GeV. The dashed and dot-dashed curves show our calculations for the contributions from W_T and W_L. The inset shows the W_L contribution on an expanded scale.

In this frame, the quark-antiquark contribution to W_Δ is completely antisymmetric in z_1 and z_2 because of the opposite sign between the $\mathcal{W}_1$ and the $\mathcal{W}_2$ terms above. The quark-gluon (or gluon-quark) contribution is proportional to $1 - z_2$ [or $(1 - z_1)$]. The asymmetry in z_1 and z_2 strongly reduces the numerical size of these contributions when $Q_\perp \neq 0$.

The combination of the quark-antiquark and antiquark-quark subprocesses gives the following perturbative contribution to W_Δ,

$$W_{q\bar{q}} + W_{\bar{q}q} \propto [q_A(\xi_1)\bar{q}_B(\xi_2) + \bar{q}_A(\xi_1)q_B(\xi_2)](z_1^2 - z_2^2). \tag{57}$$

This contribution vanishes in the central region for collisions between hadrons of the same type. The quark-gluon contribution also shows a similar asymmetry between z_1 and z_2,

$$W_{qg} + W_{gq} \propto q_A(\xi_1)g_B(\xi_2)(z_1^2 - 2z_2^2) + g_A(\xi_1)q_B(\xi_2)(2z_1^2 - z_2^2). \tag{58}$$

Collinear factorization in the perturbative calculation ceases to be valid when $Q_\perp \sim \Lambda_{\rm QCD}$ or less. At $Q_\perp = 0$, the helicity structure function W_Δ itself is ill defined. We might still be able to test the physics of the single spin-flip structure function in the small $Q_\perp$ region by introducing a new observable, for example, the first moment of the structure function,

$$\tilde{W}_\Delta(Q_T, Q) \equiv \int_0^{Q_T} dQ_\perp Q_\perp W_\Delta(Q_\perp, Q), \tag{59}$$

which is perturbatively more stable if Q_T is large enough.

Is it possible that a different kind of resummation would handle the nonphysical $Q_\perp^{-1}$ divergence at $Q_\perp = 0$ in W_Δ? We do not have an answer to this question in the collinear QCD factorization approach. However, we might gain insight by investigating the angular distribution from another perspective—starting with transverse momentum dependent quark-antiquark annihilation [3,37].

VI. SUMMARY AND DISCUSSION

Massive virtual photons, the W boson, and the Z boson have important decay modes into pairs of leptons. The angular distribution of these leptons, measured in the rest frame of the parent states, determines the alignment (polarization) of the massive vector boson and, consequently, supplies more precise information on the production dynamics than is accessible from the angular-integrated rate alone. An understanding of the expected angular distribution is also important for estimating corrections associated with limited angular acceptance in typical experiments. The changes expected in the angular distribution as a function of the transverse momentum $Q_\perp$ of the vector states is a topic of considerable interest, both for refined tests of QCD and to reduce systematic uncertainties on the determination of the W boson mass [13,14].

In this paper, we calculate the transverse momentum $Q_\perp$ dependence of the four helicity structure functions for the production of a massive pair of leptons with pair invariant mass Q. These structure functions determine the angular distribution of the leptons in the pair rest frame. We work within the QCD collinear factorization approach valid for $Q_\perp > \Lambda_{\rm QCD}$. Our goal is the prediction of the full $Q_\perp$ dependence of the four structure functions, including the region of small and intermediate $Q_\perp$ where the cross section takes on its largest values.

As also noted by others, when calculated at fixed order in QCD perturbation theory, the structure functions show unphysical inverse-power $Q_\perp^{-n}$ ($n = 1$ or 2) or logarithmic $\ln(Q/Q_\perp)$ divergences, or both, as $Q_\perp \to 0$. For the angular-integrated cross section, $d\sigma/d^4q$, it is well established that similar unphysical divergences can be removed after resummation of the $\ln^m(Q^2/Q_\perp^2)/Q_\perp^2$ singular terms from initial-state gluon emission to all orders in α_s [22–25].

We begin our analysis with the observation that the four helicity structure functions cannot be independent at $Q_\perp = 0$. The general tensor decomposition in the virtual photon rest frame in Eq. (4) is ill defined at $Q_\perp = 0$. Then, we employ electromagnetic current conservation to construct a new asymptotic hadronic tensor that has the right degrees of freedom as $Q_\perp \to 0$ and embodies the minimal divergent behavior present at fixed order in QCD perturbation theory. We find that the leading logarithmic behavior of three of the helicity structure functions, W_T, W_L, and $W_{\Delta\Delta}$, has a unique origin. Its origin is the same as that of the divergence in the angular-integrated cross section. We are able, therefore, to reduce the problem of transverse momentum resummation for W_T, W_L, and $W_{\Delta\Delta}$ to the known solution of transverse momentum resummation for the angular-integrated cross section [25]. We prove that the small $Q_\perp$ logarithmic divergences in W_T, W_L, and $W_{\Delta\Delta}$ may be resummed to all orders in the strong coupling strength α_s, yielding well-behaved predictions for the $Q_\perp$ dependences that satisfy the expected kinematic constraints at small $Q_\perp$. The fourth structure function, W_Δ, requires a different treatment, as discussed in Sec. V C.

The main results of our research include the fact that electromagnetic current conservation uniquely ties the perturbative divergences as $Q_\perp/Q \to 0$ of the otherwise independent helicity structure functions W_T, W_L, and $W_{\Delta\Delta}$ to the divergence of the angular-integrated cross section. Second, the perturbative divergence in the angular-integrated cross section is sufficient to remove all leading small $Q_\perp$ divergences of the individual helicity structure functions. Third, transverse momentum resummation of the angular-integrated cross section determines the resum-

mation of the large logarithmic terms of the helicity structure functions W_T, W_L, and $W_{\Delta\Delta}$. Finally, the approximate Lam-Tung relation between the longitudinal and the double spin-flip structure functions is an all-orders consequence of current conservation for the leading perturbatively divergent terms.

In further work, we intend to examine the $Q_\perp$ dependence of W and Z boson production, where parity violating terms introduce additional helicity structure functions. Decay of these intermediate bosons into their dilepton channels supplies accurate measurements of the masses of the bosons. For W production, more accurate predictions for the angular distribution of the single observed lepton should complement the missing energy technique and lead to an improved determination of the mass. The mass of the W boson provides an electroweak observable that bounds the mass of the Higgs boson within the framework of the standard model of particle physics [38].

The use of current conservation to establish connections between the divergences of different helicity functions at $Q_\perp \to 0$ in the Drell-Yan process may have immediate application for improving QCD resummation and predictions for particle production or other observables in SIDIS. Unlike the Drell-Yan process, the lepton angles in SIDIS cannot be integrated over fully because the measurement of the DIS kinematic variables x_B and Q^2 requires specification of the production angle of the lepton in the final state. Like the Drell-Yan cross section, the different helicity structure functions in SIDIS have a $\ln^m(Q^2/q_\perp^2)$ perturbative divergence at small values of the particle transverse momentum $q_\perp$, defined in the frame where the vector boson and the colliding hadron are aligned with each other. All helicity structure functions contribute to particle production in SIDIS. Only the leading singular $\ln^m(Q^2/q_\perp^2)/q_\perp^2$ logarithms are resummed in existing QCD calculations [29,39]. Inclusion of the effects of resummation for the individual structure functions, as described in this paper, should lead to more accurate predictions for SIDIS observables, such as particle energy flow and rapidity dependence, that could be sensitive to the relative size of the different helicity structure functions.

ACKNOWLEDGMENTS

E. L. B. is supported by the U.S. Department of Energy, Division of High Energy Physics, under Contract No. DE-AC-02-06CH11357. J-W. Q. is supported in part by the U.S. Department of Energy under Grant No. DE-FG02-87ER40371 and in part by the Argonne University of Chicago Joint Theory Institute (JTI) Grant No. 03921-07-137. R. A. R. is supported in part by the U.S. Department of Energy under Grant No. DE-FG02-87ER40371. E. L. B. thanks the Aspen Center for Physics for hospitality while part of this research was being done. We are grateful to Daniel Boer, John T. Donohue, and Werner Vogelsang for valuable communications.

APPENDIX A: DRELL-YAN CROSS SECTION AND ANGULAR DISTRIBUTION

In this appendix, we summarize the basic formalism for calculating the cross section for dilepton production in the Drell-Yan model and the angular distribution of the leptons. The expressions in this appendix also establish our notation.

We consider the scattering of two hadrons of momentum P_1 and P_2, respectively, that produces a virtual photon of four-momentum q, $A(P_1) + B(P_2) \to \gamma^*(q) + X$, that in turn decays into a pair of leptons of momentum l and $\bar{l}$, as sketched in Fig. 1. The cross section for this Drell-Yan production process can be expressed as

$$\frac{d\sigma}{d^4q\,d\Omega} = \frac{\alpha_{\rm em}^2}{2(2\pi)^4 S^2 Q^4} L_{\mu\nu} W^{\mu\nu}. \tag{A1}$$

The leptonic tensor is

$$L_{\mu\nu} = 2[l_\mu \bar{l}_\nu + l_\nu \bar{l}_\mu - l\cdot\bar{l} g_{\mu\nu}], \tag{A2}$$

and the hadronic tensor is defined as

$$\begin{aligned} W_{\mu\nu} &= S\sum_X \langle P_1P_2|J_\mu^\dagger(0)|X\rangle\langle X|J_\nu(0)|P_1P_2\rangle(2\pi)^4 \\ &\quad\times \delta^4\Big(P_1 + P_2 - q - \sum_x (p_x)\Big) \\ &= S\int d^4z e^{iq\cdot z}\langle P_1P_2|J_\mu^\dagger(0)J_\nu(z)|P_1P_2\rangle, \end{aligned} \tag{A3}$$

where J_μ is the electromagnetic current. Electromagnetic current conservation, $q^\mu W_{\mu\nu} = 0$, and the fact that electromagnetic and strong interactions are invariant under the parity and time-reversal transformation, allows us to express the Lorentz tensor, $W_{\mu\nu}$, in terms of four independent Lorentz scalar functions [4]. We choose the following four frame-independent scalar functions,

$$\begin{aligned} W^{\mu\nu} &\equiv \tilde{P}_1^\mu \tilde{P}_1^\nu \mathcal{W}_1 + \tilde{P}_2^\mu \tilde{P}_2^\nu \mathcal{W}_2 + \tfrac{1}{2}[\tilde{P}_1^\mu \tilde{P}_2^\nu + \tilde{P}_2^\mu \tilde{P}_1^\nu]\mathcal{W}_3 \\ &\quad - \tilde{g}^{\mu\nu}\mathcal{W}_4. \end{aligned} \tag{A4}$$

The dimensionless current-conserving tensor and the vectors are defined as

$$\begin{aligned} \tilde{g}^{\mu\nu} &\equiv g^{\mu\nu} - \frac{q^\mu q^\nu}{q^2}, \qquad \tilde{P}_1^\mu \equiv \tilde{g}^{\mu\nu}P_{1\nu}/\sqrt{S}, \\ &\tilde{P}_2^\mu \equiv \tilde{g}^{\mu\nu}P_{2\nu}/\sqrt{S}, \end{aligned} \tag{A5}$$

with $q_\mu \tilde{g}^{\mu\nu} = 0$. Our choice of the four frame-independent scalar functions is slightly different from that in Ref. [4]. We find that this choice is convenient for connecting to the parton-level perturbative calculation discussed below.

By contracting the leptonic tensor $L_{\mu\nu}$ and hadronic tensor $W_{\mu\nu}$ in Eq. (A1), we can express the Drell-Yan cross section in terms of the four scalar functions $\mathcal{W}_i$ and the measured hadron and lepton momenta.

The physical meaning of the scalar functions can be appreciated if we express them in terms of the four independent helicity structure functions, W_i with $i = T, L, \Delta$, and $\Delta\Delta$, corresponding to the transverse spin, longitudinal spin, single spin-flip, and double spin-flip contributions to the Drell-Yan cross section [4]. The helicity structure functions are defined in the dilepton center-of-mass frame (the virtual photon's rest frame).

The full hadronic tensor in Eq. (A4) can also be written in terms of the helicity structure functions and unit vectors in the virtual photon rest frame as in Eq. (4) [4]. In this frame, the lepton momenta are

$$\begin{aligned} l^\mu &= \frac{Q}{2}(1, \sin\theta\cos\phi, \sin\theta\sin\phi, \cos\theta), \\ \bar{l}^\mu &= \frac{Q}{2}(1, -\sin\theta\cos\phi, -\sin\theta\sin\phi, -\cos\theta). \end{aligned} \tag{A6}$$

Substituting the hadronic tensor in Eq. (4) and the leptonic tensor in Eq. (A6) into Eq. (A1), one gets the differential cross section of Eq. (1).

The frame-independent structure functions and the helicity structure functions are uniquely related to each other once we make a choice of the coordinate system, or the unit vectors, in the virtual photon rest frame. The unit vectors for the Collins-Soper frame are chosen as [26]

$$\begin{aligned} Z^\mu &= \frac{2}{\sqrt{Q^2 + Q_\perp^2}}[q_{P_2}\tilde{P}_1^\mu - q_{P_1}\tilde{P}_2^\mu], \\ X^\mu &= -\left(\frac{Q}{Q_\perp}\right)\frac{2}{\sqrt{Q^2 + Q_\perp^2}}[q_{P_2}\tilde{P}_1^\mu + q_{P_1}\tilde{P}_2^\mu], \\ Y^\mu &= \epsilon^{\mu\nu\alpha\beta}T_\nu Z_\alpha X_\beta. \end{aligned} \tag{A7}$$

The dimensionless current-conserving hadron momenta, $\tilde{P}_1^\mu$ and $\tilde{P}_1^\mu$, are defined in Eq. (A5), and $q_{P_i} \equiv P_i \cdot q/\sqrt{S}$ with $i = 1, 2$. The hadron and the virtual photon momenta can be expressed in the center-of-mass frame of the collision as

$$\begin{aligned} P_1^\mu &= \sqrt{\frac{S}{2}}\bar{n}^\mu, \qquad P_2^\mu = \sqrt{\frac{S}{2}}n^\mu, \\ q^\mu &= Q^+\bar{n}^\mu + Q^-\bar{n}^\mu + Q_\perp n_\perp^\mu, \end{aligned} \tag{A8}$$

with total center-of-mass collision energy $\sqrt{S}$, $Q^+ = \sqrt{(Q^2 + Q_\perp^2)/2}e^y$, and $Q^- = \sqrt{(Q^2 + Q_\perp^2)/2}e^{-y}$. In Eq. (A8), $\bar{n}^\mu = \delta^{\mu+}$, $n^\mu = \delta^{\mu-}$, and $n_\perp^\mu = \delta^{\mu\perp}$ are unit vectors that specify the light-cone coordinates of the collision center-of-mass frame, with $n^2 = \bar{n}^2 = 0$, $n_\perp^2 = -1$, $n \cdot \bar{n} = 1$, and $n_\perp \cdot n = n_\perp \cdot \bar{n} = 0$. In the Collins-Soper frame, the helicity structure functions can be expressed in terms of the frame-independent structure functions in Eq. (A4) as

$$\begin{aligned} W_T &= \mathcal{W}_4 + \frac{1}{2}\frac{Q_\perp^2}{Q^2}\left[\frac{1}{4}(\mathcal{W}_1 e^{-2y} + \mathcal{W}_2 e^{+2y}) + \frac{1}{4}\mathcal{W}_3\right], \\ W_L &= \frac{1}{4}(\mathcal{W}_1 e^{-2y} + \mathcal{W}_2 e^{+2y}) - \frac{1}{4}\mathcal{W}_3 + \mathcal{W}_4, \\ W_{\Delta\Delta} &= -\frac{1}{2}\frac{Q_\perp^2}{Q^2}\left[\frac{1}{4}(\mathcal{W}_1 e^{-2y} + \mathcal{W}_2 e^{+2y}) + \frac{1}{4}\mathcal{W}_3\right], \\ W_\Delta &= \frac{Q_\perp}{Q}\left[\frac{1}{4}\mathcal{W}_1 e^{-2y} - \frac{1}{4}\mathcal{W}_2 e^{+2y}\right]. \end{aligned} \tag{A9}$$

From the QCD collinear factorization formalism for the hadronic tensor in Eq. (7) we obtain similar factorized relations for structure functions,

$$W_i = \sum_{ab}\int\frac{d\xi_1}{\xi_1}\int\frac{d\xi_2}{\xi_2}\phi_a(\xi_1)\phi_b(\xi_2)w_i(\xi_1, \xi_2, q), \tag{A10}$$

with $i = T, L, \Delta\Delta, \Delta$; and

$$\mathcal{W}_i = \sum_{ab}\int\frac{d\xi_1}{\xi_1}\int\frac{d\xi_2}{\xi_2}\phi_a(\xi_1)\phi_b(\xi_2)\omega_i(\xi_1, \xi_2, q), \tag{A11}$$

with $i = 1$ 2, 3, 4. Using Eq. (A9), we derive the corresponding relation between the short-distance parton-level structure functions:

$$\begin{aligned} w_T &= \omega_4 + \frac{1}{2}\frac{Q_\perp^2}{Q^2}\left[\frac{1}{4}(\omega_1 e^{-2y} + \omega_2 e^{+2y}) + \frac{1}{4}\omega_3\right], \\ w_L &= \frac{1}{4}(\omega_1 e^{-2y} + \omega_2 e^{+2y}) - \frac{1}{4}\omega_3 + \omega_4, \\ w_{\Delta\Delta} &= -\frac{1}{2}\frac{Q_\perp^2}{Q^2}\left[\frac{1}{4}(\omega_1 e^{-2y} + \omega_2 e^{+2y}) + \frac{1}{4}\omega_3\right], \\ w_\Delta &= \frac{Q_\perp}{Q}\left[\frac{1}{4}\omega_1 e^{-2y} - \frac{1}{4}\omega_2 e^{+2y}\right]. \end{aligned} \tag{A12}$$

Integration over the solid angle of the decay leptons gives the angular-integrated Drell-Yan cross section,

$$\begin{aligned} \frac{d\sigma}{d^4q} &= \frac{\alpha_{\rm em}^2}{12\pi^3 S^2 Q^2}(2W_T + W_L) \\ &= \frac{\alpha_{\rm em}^2}{12\pi^3 S^2 Q^2}(-g_{\mu\nu}W^{\mu\nu}). \end{aligned} \tag{A13}$$

One can write the normalized Drell-Yan angular distribution as

$$\begin{aligned} \frac{dN}{d\Omega} &\equiv \left(\frac{d\sigma}{d^4q}\right)^{-1}\frac{d\sigma}{d^4q\,d\Omega} \\ &= \frac{3}{4\pi}\left(\frac{1}{\lambda + 3}\right)\Big[1 + \lambda\cos^2\theta + \mu\sin(2\theta)\cos\phi \\ &\quad + \frac{\nu}{2}\sin^2\theta\cos(2\phi)\Big], \end{aligned} \tag{A14}$$

with the coefficients of the angular dependence given by

$$\lambda = \frac{W_T - W_L}{W_T + W_L}, \qquad \mu = \frac{W_\Delta}{W_T + W_L}, \qquad \nu = \frac{2W_{\Delta\Delta}}{W_T + W_L}. \tag{A15}$$

APPENDIX B: PERTURBATIVE CONTRIBUTIONS FROM UNPOLARIZED PARTONIC STATES

In this appendix we summarize the perturbative contributions to the parton-level helicity structure functions for unpolarized initial-state partons.

Using the definition in Eq. (7), we derive the contribution to the parton-level hadronic tensor from the quark-antiquark annihilation diagrams in Fig. 2, with unpolarized initial parton states.

$$\omega^{\mu\nu}_{q\bar{q}} = \frac{4}{9} e_q^2 \frac{8\pi^2\alpha_s}{\hat{t}\,\hat{u}}[-4\xi_1^2 Q^2 S\tilde{P}_1^\mu \tilde{P}_1^\nu - 4\xi_2^2 Q^2 S\tilde{P}_2^\mu \tilde{P}_2^\nu - ((Q^2 - \hat{t})^2 + (Q^2 - \hat{u})^2)\tilde{g}^{\mu\nu}] \times S\delta(\hat{s} + \hat{t} + \hat{u} - Q^2), \tag{B1}$$

where $4/9 = (1/3)^2 \sum_A \mathrm{Tr}[t^A t^A]$ is the color factor with SU(3) generator t^A, and $8\pi^2\alpha_s = (2\pi)g_s^2$. The factor (2π) comes from the phase space expression

$$S(2\pi)^4\delta^4(p_1 + p_2 - q - p_4)\frac{d^3p_4}{(2\pi)^3 2E_4} = 2\pi S\delta(\hat{s} + \hat{t} + \hat{u} - Q^2). \tag{B2}$$

The parton-level Mandelstam variables are

$$\hat{s} = (p_1 + p_2)^2 = \xi_1\xi_2 S, \quad \hat{t} = (p_1 - q)^2 = Q^2 - 2\xi_1 P_1 \cdot q, \quad \hat{u} = (p_2 - q)^2 = Q^2 - 2\xi_2 P_2 \cdot q. \tag{B3}$$

Using Eqs. (A12) and (B1), we obtain the parton-level frame-independent structure functions

$$\begin{aligned}
\omega_1^{q\bar{q}} &= \frac{4}{9} e_q^2 \frac{8\pi^2\alpha_s}{\hat{t}\,\hat{u}}[-4\xi_1^2 Q^2 S]S\delta(\hat{s} + \hat{t} + \hat{u} - Q^2),\\
\omega_2^{q\bar{q}} &= \frac{4}{9} e_q^2 \frac{8\pi^2\alpha_s}{\hat{t}\,\hat{u}}[-4\xi_2^2 Q^2 S]S\delta(\hat{s} + \hat{t} + \hat{u} - Q^2),\\
\omega_3^{q\bar{q}} &= 0,\\
\omega_4^{q\bar{q}} &= \frac{4}{9} e_q^2 \frac{8\pi^2\alpha_s}{\hat{t}\,\hat{u}}[\xi_1^2 e^{-2y} + \xi_2^2 e^{2y}] \times [(Q^2 + Q_\perp^2)S]S\delta(\hat{s} + \hat{t} + \hat{u} - Q^2);
\end{aligned} \tag{B4}$$

and the corresponding parton-level helicity structure functions in the Collins-Soper frame,

$$\begin{aligned}
w_T^{q\bar{q}} &= \frac{4}{9} e_q^2 \frac{8\pi^2\alpha_s}{\hat{t}\,\hat{u}}[\xi_1^2 e^{-2y} + \xi_2^2 e^{2y}]S\left(Q^2 + \frac{1}{2}Q_\perp^2\right)S\delta(\hat{s} + \hat{t} + \hat{u} - Q^2),\\
w_L^{q\bar{q}} &= \frac{4}{9} e_q^2 \frac{8\pi^2\alpha_s}{\hat{t}\,\hat{u}}[\xi_1^2 e^{-2y} + \xi_2^2 e^{2y}](SQ_\perp^2)S\delta(\hat{s} + \hat{t} + \hat{u} - Q^2),\\
w_{\Delta\Delta}^{q\bar{q}} &= \frac{4}{9} e_q^2 \frac{8\pi^2\alpha_s}{\hat{t}\,\hat{u}}[\xi_1^2 e^{-2y} + \xi_2^2 e^{2y}]\left(\frac{1}{2}SQ_\perp^2\right)S\delta(\hat{s} + \hat{t} + \hat{u} - Q^2) = \frac{1}{2}w_L^{q\bar{q}},\\
w_\Delta^{q\bar{q}} &= \frac{4}{9} e_q^2 \frac{8\pi^2\alpha_s}{\hat{t}\,\hat{u}}[-\xi_1^2 e^{-2y} + \xi_2^2 e^{2y}](SQ^2)\frac{Q_\perp}{Q}S\delta(\hat{s} + \hat{t} + \hat{u} - Q^2).
\end{aligned} \tag{B5}$$

From the quark-gluon scattering diagrams in Fig. 3 with unpolarized initial parton states, we derive the quark-gluon contribution to the parton-level hadronic tensor,

$$\omega^{\mu\nu}_{qg} = \frac{1}{6} e_q^2 \frac{8\pi^2\alpha_s}{\hat{s}(-\hat{t})}[-8\xi_1^2 Q^2 S\tilde{P}_1^\mu \tilde{P}_1^\nu - 4\xi_2^2 Q^2 S\tilde{P}_2^\mu \tilde{P}_2^\nu - 4\xi_1\xi_2 Q^2 S[\tilde{P}_1^\mu \tilde{P}_2^\nu + \tilde{P}_2^\mu \tilde{P}_1^\nu] - ((Q^2 - \hat{t})^2 + (Q^2 - \hat{s})^2)\tilde{g}^{\mu\nu}]S\delta(\hat{s} + \hat{t} + \hat{u} - Q^2), \tag{B6}$$

where $1/6 = (1/3)(1/8)\sum_A \mathrm{Tr}[t^A t^A]$ is the color factor. We obtain the parton-level frame-independent structure functions

$$\begin{aligned}
\omega_1^{qg} &= \frac{1}{6} e_q^2 \frac{8\pi^2\alpha_s}{\hat{s}(-\hat{t})}[-8\xi_1^2 Q^2 S]S\delta(\hat{s} + \hat{t} + \hat{u} - Q^2),\\
\omega_2^{qg} &= \frac{1}{6} e_q^2 \frac{8\pi^2\alpha_s}{\hat{s}(-\hat{t})}[-4\xi_2^2 Q^2 S]S\delta(\hat{s} + \hat{t} + \hat{u} - Q^2),\\
\omega_3^{qg} &= \frac{1}{6} e_q^2 \frac{8\pi^2\alpha_s}{\hat{s}(-\hat{t})}[-8\xi_1\xi_2 Q^2 S]S\delta(\hat{s} + \hat{t} + \hat{u} - Q^2),\\
\omega_4^{qg} &= \frac{1}{6} e_q^2 \frac{8\pi^2\alpha_s}{\hat{s}(-\hat{t})}[\xi_1^2 e^{-2y} S(Q^2 + Q_\perp^2) + (Q^2 - \xi_1\xi_2 S)^2]S\delta(\hat{s} + \hat{t} + \hat{u} - Q^2);
\end{aligned} \tag{B7}$$

and the corresponding contribution to the parton-level helicity structure functions in the Collins-Soper frame,

$$
\begin{aligned}
w_T^{qg} &= \frac{1}{6}e_q^2\frac{8\pi^2\alpha_s}{\hat{s}(-\hat{t})}\Big[\xi_1^2 e^{-2y}SQ^2 + (Q^2-\xi_1\xi_2 S)^2 - \frac{1}{2}\frac{Q_\perp^2}{Q^2}[\xi_2^2 e^{2y} + 2\xi_1\xi_2]SQ^2\Big]S\delta(\hat{s}+\hat{t}+\hat{u}-Q^2),\\
w_L^{qg} &= \frac{1}{6}e_q^2\frac{8\pi^2\alpha_s}{\hat{s}(-\hat{t})}[2\xi_1^2 e^{-2y} + \xi_2^2 e^{2y} + 2\xi_1\xi_2](SQ_\perp^2)S\delta(\hat{s}+\hat{t}+\hat{u}-Q^2),\\
w_{\Delta\Delta}^{qg} &= \frac{1}{6}e_q^2\frac{8\pi^2\alpha_s}{\hat{s}(-\hat{t})}[2\xi_1^2 e^{-2y} + \xi_2^2 e^{2y} + 2\xi_1\xi_2]\Big(\frac{1}{2}SQ_\perp^2\Big)S\delta(\hat{s}+\hat{t}+\hat{u}-Q^2) = \frac{1}{2}w_L^{qg},\\
w_\Delta^{qg} &= \frac{1}{6}e_q^2\frac{8\pi^2\alpha_s}{\hat{s}(-\hat{t})}[-2\xi_1^2 e^{-2y} + \xi_2^2 e^{2y}]\Big(\frac{Q_\perp}{Q}\Big)(SQ^2)S\delta(\hat{s}+\hat{t}+\hat{u}-Q^2).
\end{aligned}
\tag{B8}
$$

Similarly, we derive the contributions to the parton-level hadronic tensor from the gluon-quark scattering diagrams. They are the same as those from the quark-gluon scattering diagrams with the momenta p_1 and p_2 (or equivalently with $\hat{t}$ and $\hat{u}$, and ξ_1 and ξ_2) interchanged.

APPENDIX C: PERTURBATIVE CONTRIBUTIONS FROM POLARIZED PARTONIC STATES

In this appendix we summarize the perturbative contributions to the parton-level helicity structure functions for polarized initial-state partons, defined as the states with incoming parton polarization projected onto the *difference* of the parton helicity states.

Based on the same quark-antiquark annihilation diagrams in Fig. 2, we find at this order that the contribution to the parton-level hadronic tensor from the scattering of a polarized incoming quark and antiquark is the same as that from the scattering of an unpolarized quark and antiquark,

$$\Delta\omega_{q\bar{q}}^{\mu\nu} = \omega_{q\bar{q}}^{\mu\nu}. \tag{C1}$$

On the other hand, the quark-gluon scattering diagrams in Fig. 3 with polarized quark and gluon initial states give a contribution to the parton-level hadronic tensor that differs from that for scattering of an unpolarized quark and gluon,

$$\Delta\omega_{qg}^{\mu\nu} \neq \omega_{qg}^{\mu\nu}. \tag{C2}$$

We derive

$$
\begin{aligned}
\Delta\omega_{qg}^{\mu\nu} &= \frac{1}{6}e_q^2\frac{8\pi^2\alpha_s}{\hat{s}(-\hat{t})}[+4\xi_2^2Q^2S\tilde{P}_2^\mu\tilde{P}_2^\nu\\
&\quad + 4\xi_1\xi_2Q^2S[\tilde{P}_1^\mu\tilde{P}_2^\nu + \tilde{P}_2^\mu\tilde{P}_1^\nu] - ((Q^2-\hat{t})^2\\
&\quad - (Q^2-\hat{s})^2)\tilde{g}^{\mu\nu}]S\delta(\hat{s}+\hat{t}+\hat{u}-Q^2).
\end{aligned}
\tag{C3}
$$

The contributions to the parton-level frame-independent structure functions are

$$
\begin{aligned}
\Delta\omega_1^{qg} &= 0,\\
\Delta\omega_2^{qg} &= \frac{1}{6}e_q^2\frac{8\pi^2\alpha_s}{\hat{s}(-\hat{t})}[4\xi_2^2Q^2S]S\delta(\hat{s}+\hat{t}+\hat{u}-Q^2),\\
\Delta\omega_3^{qg} &= \frac{1}{6}e_q^2\frac{8\pi^2\alpha_s}{\hat{s}(-\hat{t})}[8\xi_1\xi_2Q^2S]S\delta(\hat{s}+\hat{t}+\hat{u}-Q^2),\\
\Delta\omega_4^{qg} &= \frac{1}{6}e_q^2\frac{8\pi^2\alpha_s}{\hat{s}(-\hat{t})}[\xi_1^2e^{-2y}S(Q^2+Q_\perp^2)\\
&\quad - (Q^2-\xi_1\xi_2S)^2]S\delta(\hat{s}+\hat{t}+\hat{u}-Q^2).
\end{aligned}
\tag{C4}
$$

The corresponding contributions to the parton-level helicity structure functions in the Collins-Soper frame are

$$
\begin{aligned}
\Delta w_T^{qg} &= \frac{1}{6}e_q^2\frac{8\pi^2\alpha_s}{\hat{s}(-\hat{t})}[\xi_1^2e^{-2y}SQ^2 - (Q^2-\xi_1\xi_2S)^2 + \frac{1}{2}\frac{Q_\perp^2}{Q^2}[2\xi_1^2e^{-2y} + \xi_2^2e^{2y} + 2\xi_1\xi_2]SQ^2]S\delta(\hat{s}+\hat{t}+\hat{u}-Q^2),\\
\Delta w_L^{qg} &= \frac{1}{6}e_q^2\frac{8\pi^2\alpha_s}{\hat{s}(-\hat{t})}[-\xi_2^2e^{2y} - 2\xi_1\xi_2](SQ_\perp^2)S\delta(\hat{s}+\hat{t}+\hat{u}-Q^2),\\
\Delta w_{\Delta\Delta}^{qg} &= \frac{1}{6}e_q^2\frac{8\pi^2\alpha_s}{\hat{s}(-\hat{t})}[-\xi_2^2e^{2y} - 2\xi_1\xi_2]\Big(\frac{1}{2}SQ_\perp^2\Big)S\delta(\hat{s}+\hat{t}+\hat{u}-Q^2) = \frac{1}{2}\Delta w_L^{qg},\\
\Delta w_\Delta^{qg} &= \frac{1}{6}e_q^2\frac{8\pi^2\alpha_s}{\hat{s}(-\hat{t})}[-\xi_2^2e^{2y}]\Big(\frac{Q_\perp}{Q}\Big)(SQ^2)S\delta(\hat{s}+\hat{t}+\hat{u}-Q^2).
\end{aligned}
\tag{C5}
$$

Similarly, we derive the contribution from the polarized gluon and quark scattering process,

$$
\begin{aligned}
\Delta\omega_{gq}^{\mu\nu} &= \frac{1}{6}e_q^2\frac{8\pi^2\alpha_s}{\hat{s}(-\hat{u})}[+4\xi_1^2Q^2S\tilde{P}_1^\mu\tilde{P}_1^\nu + 4\xi_1\xi_2Q^2S[\tilde{P}_1^\mu\tilde{P}_2^\nu + \tilde{P}_2^\mu\tilde{P}_1^\nu]\\
&\quad - ((Q^2-\hat{u})^2 - (Q^2-\hat{s})^2)\tilde{g}^{\mu\nu}]S\delta(\hat{s}+\hat{t}+\hat{u}-Q^2).
\end{aligned}
\tag{C6}
$$

The contributions to the parton-level frame-independent structure functions are

$$\begin{aligned}
\Delta\omega_1^{gq} &= \frac{1}{6}e_q^2\frac{8\pi^2\alpha_s}{\hat{s}(-\hat{u})}[4\xi_1^2Q^2S]S\delta(\hat{s}+\hat{t}+\hat{u}-Q^2),\\
\Delta\omega_2^{gq} &= 0,\\
\Delta\omega_3^{gq} &= \frac{1}{6}e_q^2\frac{8\pi^2\alpha_s}{\hat{s}(-\hat{u})}[8\xi_1\xi_2Q^2S]S\delta(\hat{s}+\hat{t}+\hat{u}-Q^2),\\
\Delta\omega_4^{gq} &= \frac{1}{6}e_q^2\frac{8\pi^2\alpha_s}{\hat{s}(-\hat{u})}[\xi_2^2\mathrm{e}^{2y}S(Q^2+Q_\perp^2)-(Q^2-\xi_1\xi_2S)^2]S\delta(\hat{s}+\hat{t}+\hat{u}-Q^2).
\end{aligned} \tag{C7}$$

The corresponding contributions to the parton-level helicity structure functions in the Collins-Soper frame are

$$\begin{aligned}
\Delta w_T^{gq} &= \frac{1}{6}e_q^2\frac{8\pi^2\alpha_s}{\hat{s}(-\hat{u})}[\xi_2^2\mathrm{e}^{2y}SQ^2-(Q^2-\xi_1\xi_2S)^2+\frac{1}{2}\frac{Q_\perp^2}{Q^2}[\xi_1^2\mathrm{e}^{-2y}+2\xi_2^2\mathrm{e}^{2y}+2\xi_1\xi_2]SQ^2]S\delta(\hat{s}+\hat{t}+\hat{u}-Q^2),\\
\Delta w_L^{gq} &= \frac{1}{6}e_q^2\frac{8\pi^2\alpha_s}{\hat{s}(-\hat{u})}[-\xi_1^2\mathrm{e}^{-2y}-2\xi_1\xi_2](SQ_\perp^2)S\delta(\hat{s}+\hat{t}+\hat{u}-Q^2),\\
\Delta w_{\Delta\Delta}^{gq} &= \frac{1}{6}e_q^2\frac{8\pi^2\alpha_s}{\hat{s}(-\hat{u})}[-\xi_1^2\mathrm{e}^{-2y}-2\xi_1\xi_2]\left(\frac{1}{2}SQ_\perp^2\right)S\delta(\hat{s}+\hat{t}+\hat{u}-Q^2)=\frac{1}{2}\Delta w_L^{gq},\\
\Delta w_\Delta^{gq} &= \frac{1}{6}e_q^2\frac{8\pi^2\alpha_s}{\hat{s}(-\hat{u})}[\xi_1^2\mathrm{e}^{-2y}]\left(\frac{Q_\perp}{Q}\right)(SQ^2)S\delta(\hat{s}+\hat{t}+\hat{u}-Q^2).
\end{aligned} \tag{C8}$$

[1] S. D. Drell and T. M. Yan, Phys. Rev. Lett. **25**, 316 (1970); **25**, 902(E) (1970).
[2] See, for example, G. E. Hogan *et al.*, Phys. Rev. Lett. **42**, 948 (1979); K. J. Anderson *et al.*, Phys. Rev. Lett. **43**, 1219 (1979); J. Badier *et al.*, Z. Phys. C **11**, 195 (1981), and references therein.
[3] E. L. Berger, J. T. Donohue, and S. Wolfram, Phys. Rev. D **17**, 858 (1978); J. T. Donohue, in *Proceedings of Phenomenology of Quantum Chromodynamics, Moriond, 1978*, edited by J. Tran Thanh Van (Editions Frontieres, Dreux, France, 1978), Vol. I, pp. 159–163.
[4] C. S. Lam and W. K. Tung, Phys. Rev. D **18**, 2447 (1978).
[5] K. Kajantie, J. Lindfors, and R. Raitio, Phys. Lett. **74B**, 384 (1978); J. Lindfors, Phys. Scr. **20**, 19 (1979).
[6] J. Cleymans and M. Kuroda, Phys. Lett. **80B**, 385 (1979); **86B**, 426(E) (1979); Nucl. Phys. **B155**, 480 (1979); **B160**, 510(E) (1979).
[7] C. S. Lam and W. K. Tung, Phys. Rev. D **21**, 2712 (1980).
[8] J. C. Collins, Phys. Rev. Lett. **42**, 291 (1979).
[9] E. Mirkes, Nucl. Phys. **B387**, 3 (1992); E. Mirkes and J. Ohnemus, Phys. Rev. D **51**, 4891 (1995).
[10] P. Chiappetta and M. Le Bellac, Z. Phys. C **32**, 521 (1986).
[11] D. Boer and W. Vogelsang, Phys. Rev. D **74**, 014004 (2006).
[12] G. Bunce *et al.*, "Status and Prospects of the RHIC Spin Physics Program," http://spin.rhic.bnl.gov/rsc/report/masterspin.pdf, 2007.
[13] C. Balazs, J. W. Qiu, and C. P. Yuan, Phys. Lett. B **355**, 548 (1995).
[14] R. K. Ellis, D. A. Ross, and S. Veseli, Nucl. Phys. **B503**, 309 (1997).
[15] S. Falciano *et al.* (NA10 Collaboration), Z. Phys. C **31**, 513 (1986).
[16] M. Guanziroli *et al.* (NA10 Collaboration), Z. Phys. C **37**, 545 (1988).
[17] J. S. Conway *et al.*, Phys. Rev. D **39**, 92 (1989).
[18] J. G. Heinrich *et al.*, Phys. Rev. D **44**, 1909 (1991).
[19] L. Y. Zhu *et al.* (FNAL-E866/NuSea Collaboration), Phys. Rev. Lett. **99**, 082301 (2007).
[20] E. L. Berger and S. J. Brodsky, Phys. Rev. Lett. **42**, 940 (1979).
[21] J. W. Qiu and G. Sterman, Nucl. Phys. **B353**, 105 (1991).
[22] Y. L. Dokshitzer, D. Diakonov, and S. I. Troian, Phys. Rep. **58**, 269 (1980).
[23] G. Parisi and R. Petronzio, Nucl. Phys. **B154**, 427 (1979).
[24] J. C. Collins and D. E. Soper, Nucl. Phys. **B193**, 381 (1981); **B213**, 545(E) (1983).
[25] J. C. Collins, D. E. Soper, and G. Sterman, Nucl. Phys. **B250**, 199 (1985), and references therein.
[26] J. C. Collins and D. E. Soper, Phys. Rev. D **16**, 2219 (1977).
[27] E. L. Berger, J. W. Qiu, and R. A. Rodriguez-Pedraza, arXiv:0707.3150 [Phys. Lett. B (to be published)].
[28] J. C. Collins, D. E. Soper, G. Sterman, Adv. Ser. Dir. High Energy Phys. **5**, 1 (1988), and references therein.
[29] R. Meng, F. I. Olness, and D. E. Soper, Phys. Rev. D **54**, 1919 (1996); Nucl. Phys. **B371**, 79 (1992).
[30] R. A. Rodriguez-Pedraza, Ph.D. dissertation, Iowa State University.
[31] F. Landry, R. Brock, G. Ladinsky, and C. P. Yuan, Phys.

Rev. D **63**, 013004 (2000); F. Landry, R. Brock, P. M. Nadolsky, and C. P. Yuan, Phys. Rev. D **67**, 073016 (2003).

[32] J. W. Qiu and X. F. Zhang, Phys. Rev. Lett. **86**, 2724 (2001); Phys. Rev. D **63**, 114011 (2001).

[33] E. L. Berger, L. E. Gordon, and M. Klasen, Phys. Rev. D **58**, 074012 (1998).

[34] J. W. Qiu, R. Rodriguez, and X. F. Zhang, Phys. Lett. B **506**, 254 (2001).

[35] E. L. Berger, J. W. Qiu, and X. F. Zhang, Phys. Rev. D **65**, 034006 (2002).

[36] P. L. McGaughey *et al.* (E772 Collaboration), Phys. Rev. D **50**, 3038 (1994); **60**, 119903(E) (1999).

[37] X. D. Ji, J. P. Ma, and F. Yuan, Phys. Lett. B **597**, 299 (2004); Phys. Rev. D **71**, 034005 (2005).

[38] T. Aaltonen *et al.* (CDF Collaboration), arXiv:0707.0085 [Phys. Rev. Lett. (to be published)], and references therein.

[39] P. Nadolsky, D. R. Stump, and C. P. Yuan, Phys. Rev. D **61**, 014003 (1999); **64**, 059903(E) (2001); **64**, 114011 (2001); Phys. Lett. B **515**, 175 (2001).